

MicroRNAs miR-25, let-7 and miR-124 regulate the neurogenic potential of Müller glia in mice

Stefanie G. Wohl^{1,2,*}, Marcus J. Hooper¹ and Thomas A. Reh¹

ABSTRACT

Müller glial cells (MG) generate retinal progenitor (RPC)-like cells after injury in non-mammalian species, although this does not occur in the mammalian retina. Studies have profiled gene expression in these cells to define genes that may be relevant to their differences in neurogenic potential. However, less is known about differences in micro-RNA (miRNA) expression. In this study, we compared miRNAs from RPCs and MG to identify miRNAs more highly expressed in RPCs, and others more highly expressed in MG. To determine whether these miRNAs are relevant to the difference in neurogenic potential between these two cell types, we tested them in dissociated cultures of MG using either mimics or antagomiRs to increase or reduce expression, respectively. Among the miRNAs tested, miR-25 and miR-124 overexpression, or let-7 antagonism, induced *Ascl1* expression and conversion of ~40% of mature MG into a neuronal/RPC phenotype. Our results suggest that the differences in miRNA expression between MG and RPCs contribute to their difference in neurogenic potential, and that manipulations in miRNAs provide a new tool with which to reprogram MG for retinal regeneration.

KEY WORDS: Retina, Reprogramming, miRNAs, Single cell RNA-seq, *Ascl1*, Adult

INTRODUCTION

In fish and birds, Müller glial cells (MG) respond to injury of the retina by re-entering the cell cycle and generating retinal progenitor-like cells, and ultimately new neurons. In fish, the ability of MG to generate new retinal progenitor cells (RPCs) is in part controlled by miRNAs (for a review, see Goldman, 2014). Retinal injury in fish induces the RNA-binding protein Lin28, which functions to reduce levels of the miRNA let-7 and allow expression of *Ascl1*, which is crucial for regeneration in these species (Ramachandran et al., 2010; for a review, see Goldman, 2014). In addition, the downregulation of another miRNA in fish, miR-203, has been reported to increase proliferation of progenitors and is required for retinal regeneration after light damage (Rajaram et al., 2014).

Although mammalian retinas also have MG, unlike the fish, MG in the mammalian retina do not naturally generate RPCs in response to injury (Karl and Reh, 2010; Löffler et al., 2015; Ueki et al., 2015; Wilken and Reh, 2016; Karl et al., 2008; Löffler et al., 2015; Ueki et al., 2015; Wilken and Reh, 2016). The analysis of differences in gene expression between mammalian MG and RPCs

(Blackshaw et al., 2004; Brzezinski et al., 2011; Nelson et al., 2011) revealed a set of transcription factor candidates that were subsequently tested in dissociated cell cultures of MG to determine their potential for reprogramming mouse MG to the RPC state. We found that *Ascl1* overexpression activated RPC genes and subsequent neuron differentiation in dissociated cultures of mouse MG (Pollak et al., 2013). This same transcription factor (in conjunction with a HDAC inhibitor) was also effective at stimulating functional regeneration of neurons *in vivo* (Jorstad et al., 2017; Ueki et al., 2015). Similar studies of other candidate reprogramming factors further demonstrated that miRNAs miR-124, miR-9 and miR-9* (alone or in combination with *Ascl1*) (Wohl and Reh, 2016b) were effective in stimulating the conversion of mouse MG to RPCs and/or neurons. However, a comprehensive survey of miRNAs that differ between progenitors and glia, similar to that carried out for mRNAs, has not been reported.

We therefore used fluorescence-activated cell sorting (FACS) to purify RPCs from postnatal day 2 mice and MG from P8, P11 and adult mice. The RNA was extracted from purified RPCs and MG, and miRNA expression was analyzed by means of the molecular barcode technology called NanoStrings (Dennis et al., 2015; Geiss et al., 2008). We identified the miRNAs that were more highly expressed in RPCs, when compared with MG, as well as miRNAs that were more highly expressed in MG than in RPCs. For the miRNAs that were enriched in the FACS-purified RPCs when compared with the MG, we experimentally overexpressed these in MG cultures to determine whether neurogenic competency could be restored. Similarly, for miRNAs that were enriched in the MG relative to the RPCs, we antagonized these in the MG to determine whether this would restore neurogenic competency to the MG. We found that manipulations in two miRNAs, miR-25 (mimic) and let-7 (antagomiR), stimulated neural reprogramming of MG with a neuronal conversion of up to 40% of young MG *in vitro*. The combination of miR-25 overexpression and let-7 inhibition was even more effective than either treatment alone, with ~60% of the *Ascl1*-expressing MG developing neuronal phenotypes. This reprogramming capacity was decreased in adult MG cultures (range 1-4 months) to ~20%. Single cell RNA-seq of reprogrammed MG confirmed that many of the cells acquired a gene expression profile similar to RPCs and retinal neurons. Together, our data show that miRNAs are important in regulating the development of MG, and at least one of these, let-7, has a conserved role in the neurogenic competence of both mouse and fish MG.

RESULTS

The miRNA profile of retinal progenitor cells and Müller glia in the mouse retina

We have previously reported miRNA expression in MG, using FACS to purify the cells from mature retina (Wohl and Reh, 2016a). To determine which miRNAs are uniquely expressed in RPCs, we

¹Department of Biological Structure, University of Washington, School of Medicine, Seattle, WA 98195, USA. ²Department of Biological and Vision Sciences, The State University of New York, College of Optometry, New York, NY 10036, USA.

*Author for correspondence (swohl@sunyopt.edu)

© S.G.W., 0000-0003-2559-7678; M.J.H., 0000-0003-1228-5958; T.A.R., 0000-0002-3524-0886

used a similar strategy and FACS-purified RPCs from postnatal day 2 (P2) Sox2-CreER: tdTomato^{flSTOP/flSTOP} mice. We induced expression of the reporter by tamoxifen injections at P0 and P1, resulting in tdTomato expression in many cells of the neuroblastic layer (NBL). The majority of these cells also expressed progenitor markers Sox9 and Sox2. The fraction of the tdTomato⁺ cells was ~50% of the total, somewhat higher than expected (Fig. S1A,A',F). In addition to the RPCs, it is likely that some of the tdTomato⁺ cells were also the neuronal progeny of the RPCs. Moreover Sox2-CreER is also expressed in a small number of amacrine cells (Fig. S1A,E). These two Sox2⁺ populations thus reduce the purity of the final sample. To label MG, we used a different strategy that allowed for greater purity of the cells. We FACS purified the MG at the ages P8, P11 and >P21 from Rbp1-CreER:tdTomato^{flSTOP/flSTOP} mice, as previously described (Wohl et al., 2017; Wohl and Reh, 2016a). After tamoxifen application, the majority of MG [Sox9, Sox2 and glutamine synthetase (GS)] were labeled; the MG represented

1.5–2.1% of all cells (Fig. S1B–D',F), consistent with previous estimates of MG in the mouse retina (Grosche et al., 2016; Jeon et al., 1998).

To quantify the miRNAs expressed in RPCs and MG, total RNA was extracted from FACS-purified Sox2:tdTomato⁺ and Rbp1:tdTomato⁺ cells. The miRNAs were measured by solution hybridization using the NanoString nCounter assay (Geiss et al., 2008). The expression profiles of RPCs and MG are shown in Fig. 1A as a heatmap of all ages. We found three main clusters, a green cluster with miRNAs moderately expressed, a blue cluster with miRNAs with low expression and a pink cluster with the most highly expressed miRNAs. A list of the miRNAs in each of the three clusters can be found in Table S1. Interestingly, the overall miRNA expression profiles of RPCs and MG are quite similar, in accordance with the known similarity in the transcriptome of these cells (Jadhav et al., 2009; Roesch et al., 2008). To better visualize the miRNAs differentially expressed between RPCs and

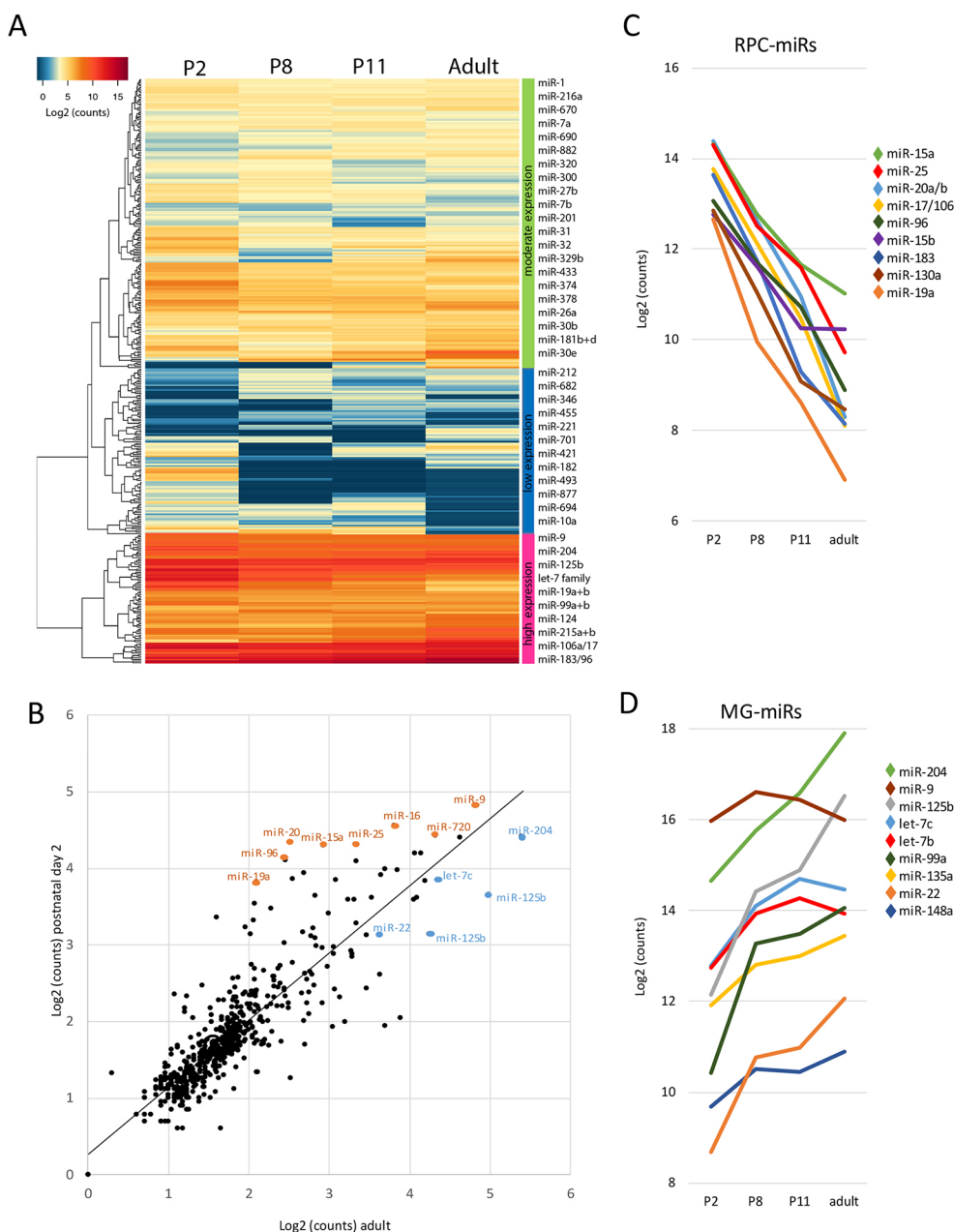


Fig. 1. MicroRNAs highly expressed in RPCs and MG. (A) Heatmap of the results of a hierarchical clustering of the most highly expressed miRNAs [Log2 (counts)] across all ages in the RPCs (P2) and MG (P8, P11 and adult). The miRNAs in the three main clusters (green, blue and pink) are listed in Table S1. (B) Scatter plot of Log2 counts of the miRNAs from RPCs and adult MG. All miRNAs expressed above the black line are miRNAs more highly expressed in RPCs than in MG, with the top progenitor miRNAs highlighted in orange. All miRNAs below the black line are miRNAs more highly expressed in MG than in RPCs, with the top MG miRNAs highlighted in blue. (C) Time course of expression of nine miRNAs whose levels increase the most from P2 to adult (RPC-miRs). (D) Time course of 11 miRNAs that are highly expressed in RPCs and decline during MG maturation. The sorts of all retinas per age were pooled for the data shown (P2, 4 mice; P8, 26 mice; P11, 16 mice; adult, 40 mice).

mature MG, we plotted the miRNA expression levels of P2 RPCs and adult MG as a scatterplot, shown in Fig. 1B (the top 25 miRNAs can be found in Table S2; miRNAs expressed more highly in RPCs than in MG are above the line, whereas miRNAs expressed more highly in MG than RPCs are below the line). Of 600 miRNAs analyzed, we focused on 11 that were both highly expressed and had substantially lower levels of expression in RPCs than in MG (Fig. 1C). Among the miRNAs more highly expressed in RPCs were members of the miR-17 family, i.e. miR-106/miR-17, miR-20a/b, miR-15a/b, miR-19a and miR-25. These miRNAs are in three clusters in the mouse genome and may be transcribed together. Several of these miRNAs have already been implicated in neurogenesis and cell proliferation in other areas of the nervous system (Beveridge et al., 2009; Foshay and Gallicano, 2009; Jin et al., 2016, 2018; Mao et al., 2014; Naka-Kaneda et al., 2014; Trompeter et al., 2011; Yang et al., 2017). By contrast, the nine most highly expressed miRNAs that had the greatest increase from P2 RPCs to P8 or older MG included miR-204, miR-125b, members of the let-7 family (let-7c and let-7b) and the related miRNA miR-99a (Fig. 1D).

let-7 antagonists and miR-25 mimics induce Ascl1-reporter expression in MG

To test whether miRNAs regulate the neurogenic competence of MG, we used primary dissociated cell cultures, as this method has proven effective for identifying reprogramming factors that are effective both *in vitro* and *in vivo* (Jorstad et al., 2017; Pollak et al., 2013; Ueki et al., 2015). We hypothesized that miRNAs highly expressed in RPCs may be important in establishing and maintaining the RPC gene expression pattern. One prediction of this hypothesis is that overexpression of the RPC-miRNAs in MG would cause the MG to adopt a progenitor-like gene expression profile. To test this prediction, we transfected dissociated cultures of MG with miRNA mimics (double-stranded, preprocessed miRNAs). For the initial screen, we used MG cultured from Ascl1-CreER:tdTomato^{flSTOP/flSTOP} reporter mice, to label cells that express the progenitor gene Ascl1 (Fig. 2A). Out of the most highly expressed RPC miRNAs (i.e. high in RPCs but low in MG), we used one candidate from every family (i.e. containing the same seed sequence Fig. S2A). Specifically, we tested mimics for miR-15a, miR-17, miR-19a and miR-25. We included miR-124 as a positive control, as our previous report demonstrated that this miRNA also induces Ascl1 expression and neuronal gene expression in MG (Wohl and Reh, 2016b). Two other miRNAs that were more highly expressed in the RPC sample than in the MG samples were miR-183 and miR-96. These have been previously localized to photoreceptors (Busskamp et al., 2014; Xiang et al., 2017; Xu et al., 2007; Zhu et al., 2011), and possibly represent a contaminating population of photoreceptors in the P2 RPC population. These were not tested in this assay.

MG cultures from P11 Ascl1-CreER:tdTomato^{flSTOP/flSTOP} mice were transfected with either a cocktail of all four RPC-miR mimics, or each miRNA mimic individually (Fig. 2B). We added 4-hydroxytamoxifen to the cultures to activate the cre-recombinase and monitored the cells for tdTomato expression. After 4 days post-transfection, we found a few cells expressing the reporter in control MG (Fig. 2C). By contrast, the cocktail of all four RPC-miRNAs (Fig. 2D), miR-25 alone (Fig. 2E) as well as miR-124 (Fig. S2B) led to a significant increase in the number of Ascl1:tdTomato⁺ cells (Fig. 2I). miR-15a, miR-17 and miR-19a, however, did not cause an increase in the number of reporter positive cells. After 6–8 days post transfection, some Ascl1:tdTomato⁺ cells transfected with either the

RPC-cocktail or miR-25 alone underwent morphological changes and took on a more neuronal-like morphology, with small somata and long processes (Fig. 2C'–E', Fig. S2C). As miR-25 alone had a similar effect to the RPC-cocktail, we used miR-25 alone in additional experiments.

Next, we focused on the miRNAs whose levels increase with glial maturation. The miRNAs expressed more highly in MG than RPCs included the previously described mGliomiRs miR-204, miR-125, miR-9, miR-99a and miR-135a, as well as miR-22, miR-148a, let-7a and let-7c. We hypothesized that the increase in these miRNAs in MG might prevent them from expressing progenitor genes. One prediction of this hypothesis is that antagonism of these miRNAs would promote RPC gene expression and neuron differentiation. To test this prediction, we used complementary hairpin inhibitors called antagonists (AR). We tested these miRNA ARs either alone or in combination (Fig. S3A–C). Interestingly, the only AR that induced the Ascl1 reporter was let-7AR (either let-7a or let-7c, Fig. 2F,J), and only after let-7 inhibition did we observe cells with a neuronal morphology (~40%, Fig. 2F', Fig. S3A,D), similar to the effect of miR-25 mimic overexpression.

We then combined both approaches: cells were transfected with miR-25 mimic and let-7AR, with or without miR-124, in MG cultures from the Ascl1 reporter mice to determine whether the combination was more effective than either manipulation alone (Fig. 2G,H). The combination of miR-25, let-7AR and miR-124 led to a further increase of Ascl1 expression in the MG (Fig. 2G,H,K). In addition, in the controls (control mimics and control antagonists combined) Ascl1:tdTomato⁺ displayed a flat cell morphology, whereas Ascl1:tdTomato cells treated with miR-25+let-7AR or miR-25+let-7AR+miR-124 mimics adopted a neuronal morphology, with a small somata and various fine processes (Fig. 2G',H'). In all of the combinations, there were more Ascl1:tdTomato⁺ cells and a larger fraction of neuronal-like cells (50–60%) compared with in the single treatments (Fig. S3E).

let-7 antagonists and miR-25 mimics reprogram MG to neural progenitors and neurons

In order to confirm the neuronal identity of the cells in the miR-treated conditions, Map2 and Otx2 immunofluorescent labeling and confocal microscopy were carried out (Fig. 3). Many of the Ascl1:tdTomato⁺ neuronal-like cells were positive for Map2 and they accounted for 52–54% of all Ascl1:tdTomato⁺ cells (Fig. 3C–G). These neuronal cells were either highly branched or had one long process with a growth cone-like structure. (Fig. 3F, arrowhead and arrows, respectively). Approximately 44% of the miR-25/let-7AR-transfected cells expressed Otx2, with close to 30% expressing both Map2 and Otx2. Slightly higher percentages of neuronal-like cells were obtained in the miR-25/miR-124/let-7AR transfected cells, with almost 60% of the Ascl1:tdTomato⁺ cells expressing Otx2 and 40% being positive for both Map2 and Otx2 (Fig. 3H,I). Although the percentages of Map2⁺ (35–62%), Otx2⁺ (20–38%) and Map2⁺/Otx2⁺ cells (10–20%) in the single treatments were also high, the overall number of neurons was lower than in the cocktail-treated wells (Fig. S4). These results extend our previous observations with miR-124 and show that the combination of miR-25 overexpression and let-7 inhibition, with or without miR-124 overexpression, leads to a significant increase in Ascl1-expressing MG *in vitro*, with approximately half of the Ascl1:tdTomato⁺ expressing Map2 and/or Otx2.

The use of the Ascl1 reporter allowed us to determine whether miRNAs can induce the expression of this reporter in MG; however, to further confirm that the new neurons were indeed derived from

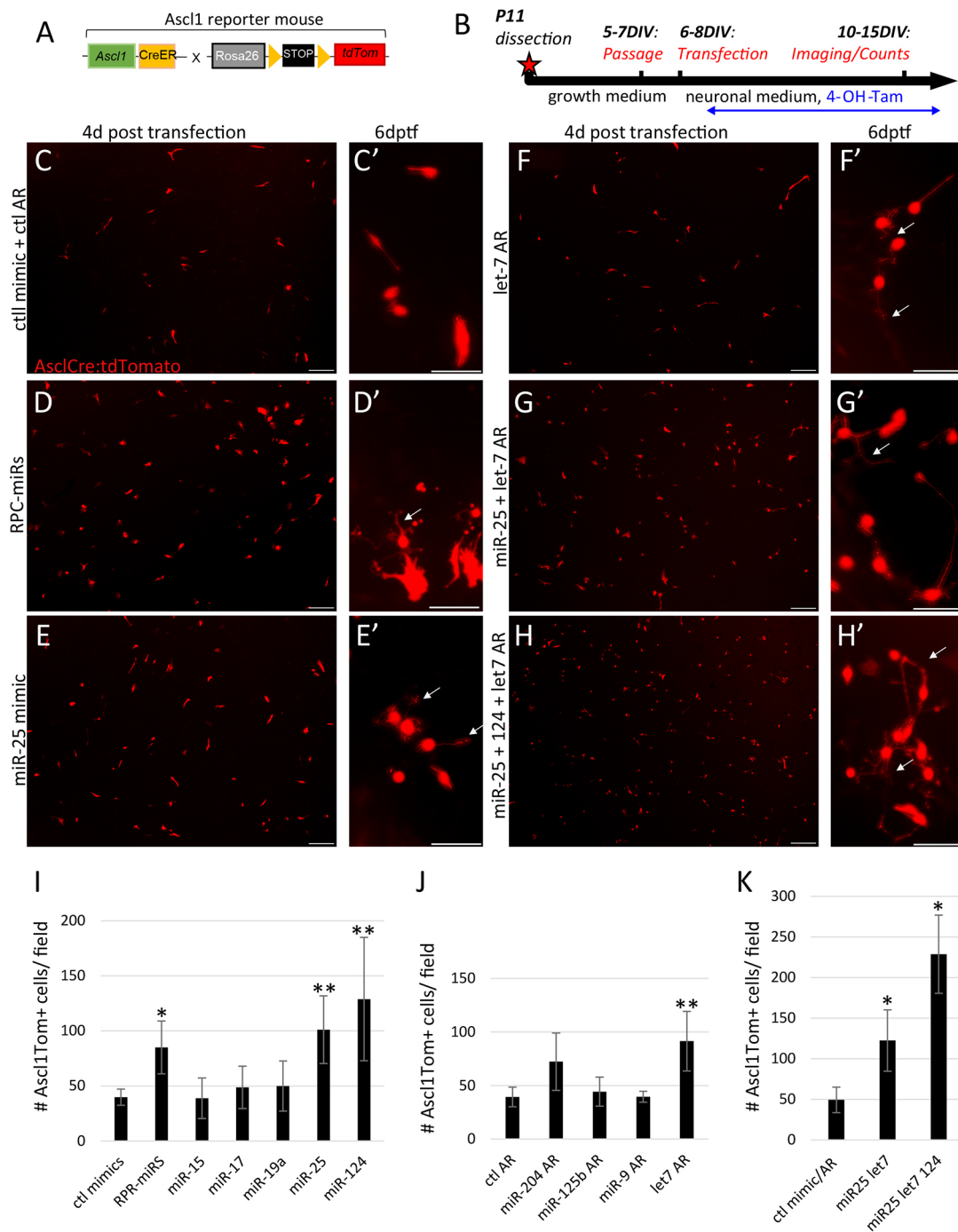


Fig. 2. Overexpression of miR-25 and/or antagonism of let-7 induces *Ascl1* expression in MG. (A) Schematic of the *Ascl1*^{CreER}: *tdTomato*^{flSTOP/flSTOP} construct. (B) Experimental design. (C-H') Live images of *tdTomato*⁺ cells after transfection with control (C,C'), RPC-miR cocktail (D,D'), miR-25 mimic (E,E'), let-7 antagoniR (AR, F,F'), miR-25 and let-7 AR (G,G') or miR-25 and miR-124 mimic and let-7 AR (H,H') 4 days post transfection (dptf). Arrows indicate cells with fine processes. (I-K) Number of *Ascl1**tdTomato*⁺ cells per field at 3-5 dptf with single or combined RPC-miR mimics (I, $n \geq 3$), single MG-miR antagoniRs (AR, J, $n \geq 3$) or miR-25 mimics combined with let-7 AR, with or without miR-124 mimic (K, $n \geq 5$). Scale bars: 200 μ m in C-H; 100 μ m in C'-H'. Significant differences of each treatment group from control wells are indicated: * $P < 0.05$, ** $P < 0.01$, Mann-Whitney test. n , number of cultures of six to eight mice per culture. ctl, control.

MG, we used an additional reporter mouse line, the *Rlbp1*-*CreER*: *tdTomato*^{flSTOP/flSTOP} MG reporter, for the next series of experiments (Fig. 4A). This line has been extensively characterized; the *Rlbp1*-*CreER* is expressed in all MG, but not neurons or astrocytes at postnatal day 8 or older (Wohl et al., 2017). In this line of mice, all MG express the reporter, so visualization of individual cells in the

cultures is difficult. Therefore, we used the following strategy to label only one-third of the MG: P11 retinas from the *Rlbp1*-*CreER*: *tdTomato* mice were dissociated and plated as usual, but 4-hydroxytamoxifen was added to only two out of six wells to induce reporter transgene expression. When the cells were passaged, the *tdTomato*-expressing cells were combined with the untreated

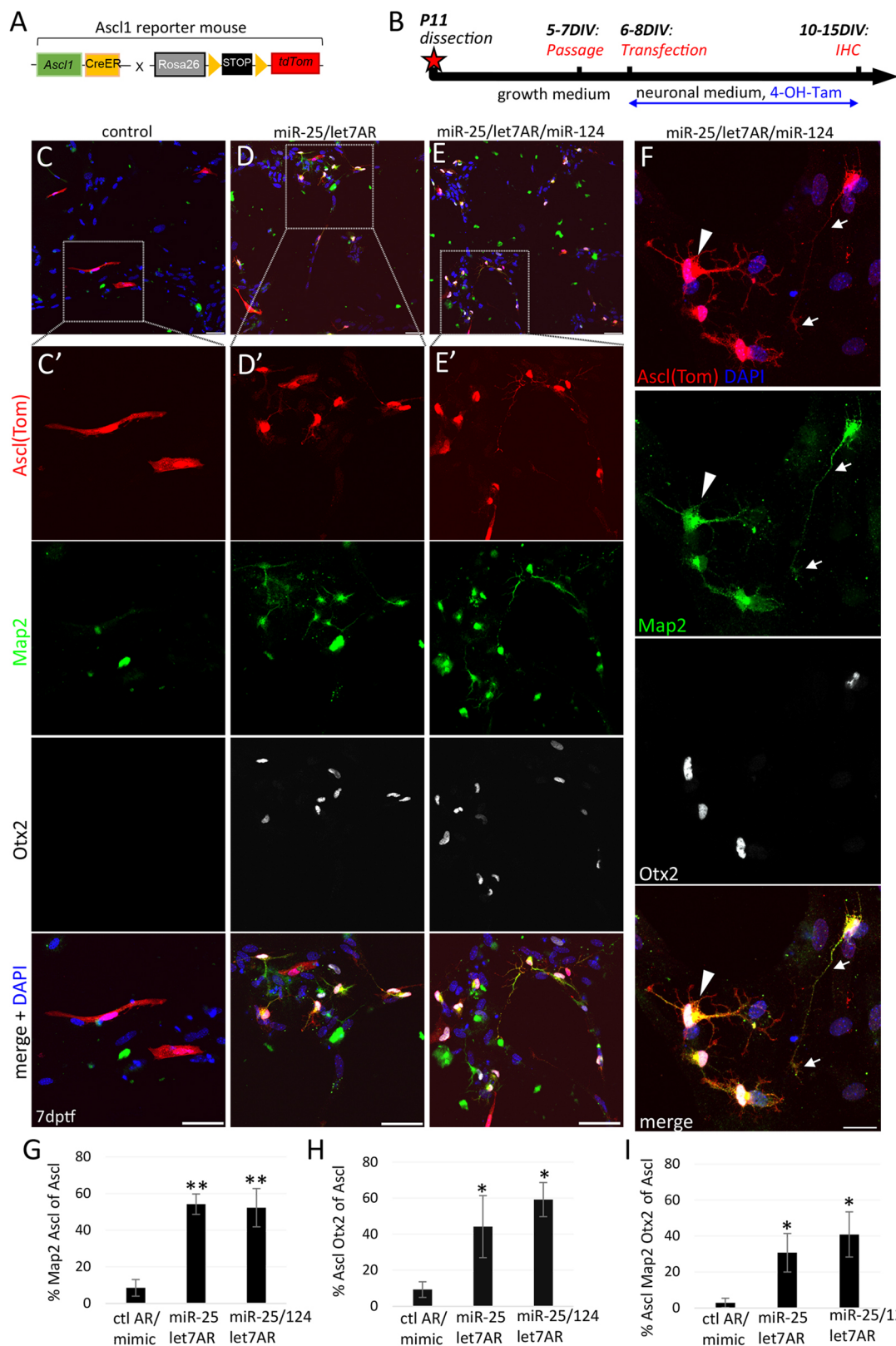


Fig. 3. miR-25/miR-124/let-7 reprogrammed Ascl1-expressing MG express Map2 and Otx2. (A) Ascl1-tdTomato reporter construct. (B) Experimental design. (C-F) Immunofluorescent labeling for tdTomato (AsclTom), Map2 and Otx2, as well as DAPI nuclear labeling, 7 days post transfection (7 dptf). Map2⁺Otx2⁺ neurons are either highly branched (arrowhead in F) or have one long process with a growth cone-like structure (arrows). (G) Percentage of AsclTom⁺Map2⁺ cells out of total AsclTom⁺ cells at 7 dptf (n=6). (H) Percentage of AsclTom⁺Otx2⁺ cells out of total AsclTom⁺ cells 7 dptf (n=4). (I) Percentage of Map2⁺Otx2⁺AsclTom⁺ cells/AsclTom⁺ cells at 7 dptf (n=3). Scale bars: 100 μ m in C,D,E; 50 μ m in C',D',E'; 20 μ m in F. Significant differences for each treatment condition from control wells are indicated. * P <0.05, ** P <0.01 (for G,H, Mann-Whitney-test; for I, Levene's test for variances and t -test). n , number of cultures of six to eight mice per culture. ctl, control.

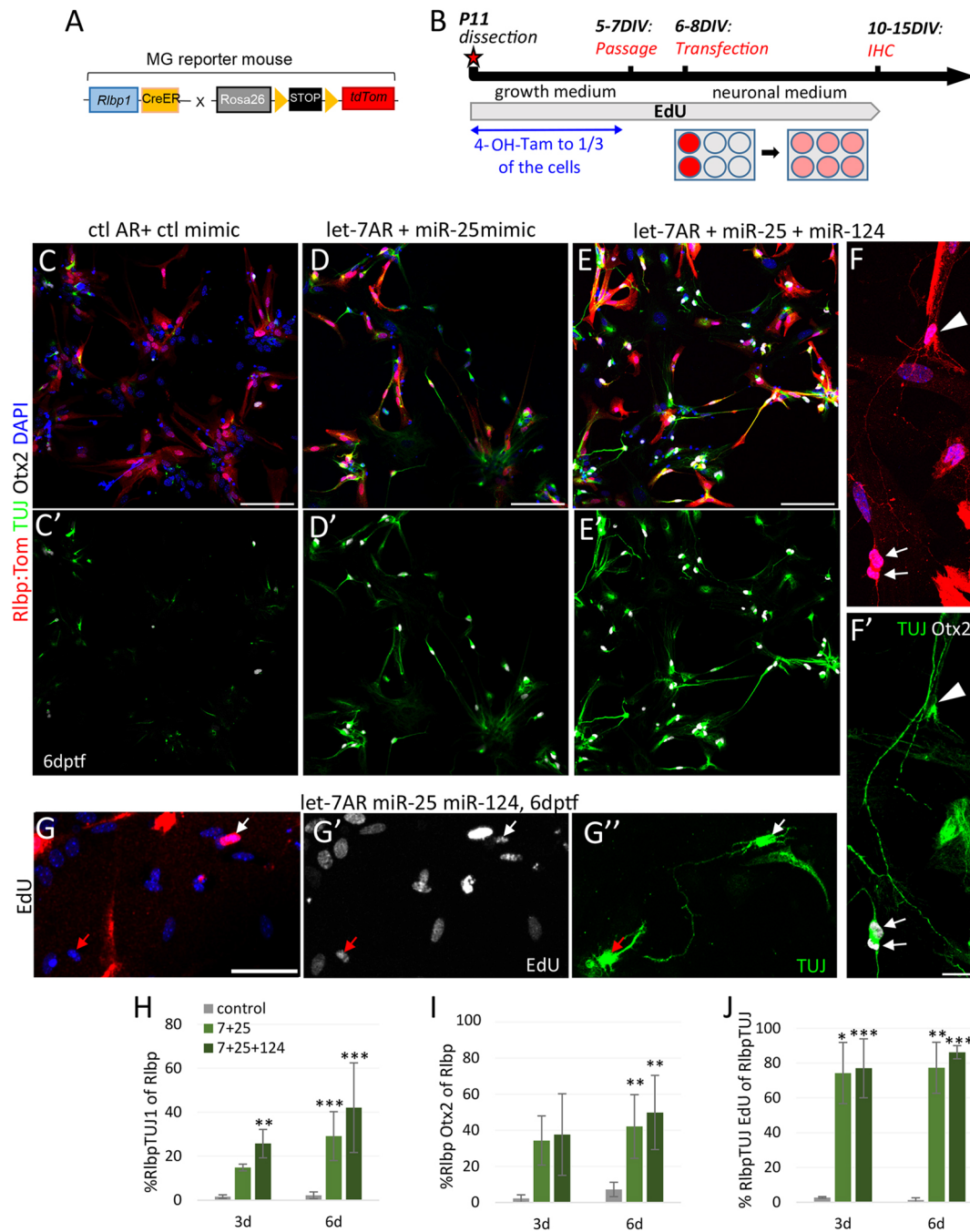


Fig. 4. miR-25/miR-124/let-7 reprogrammed Rlbp1⁺ MG express TUJ and Otx2. (A) Schematic of the *Rlbp1CreER*: *tdTomato*^{flSTOP/STOP} construct. (B) Experimental design. (C–G'') Immunofluorescent labeling for tdTomato (Rlbp1), TUJ1 and Otx2 or EdU (G–G''), as well as DAPI nuclear labeling, 6 days post transfection (dptf). The arrowhead in F,F' shows an Otx2[−] cell; the arrows in F,F' show Otx2⁺ neurons. The red arrow in G–G'' shows a BrdU[−] neuron; the white arrow in G–G'' shows a BrdU⁺ neuron. (H) Percentage of TUJ1⁺Rlbp:tdTomato⁺ cells out of total Rlbp:tdTomato⁺ cells at 3 dptf (*n*=3) and 6 dptf (*n*=8). (I) Percentage of Otx2⁺Rlbp:tdTomato⁺ cells out of total Rlbp:tdTomato⁺ cells at 3 dptf (*n*=3) and 6 dptf (*n*=6). (J) Percentage of TUJ1⁺EdU⁺Rlbp:tdTomato⁺ cells out of total Rlbp:tdTomato⁺ cells at 3 dptf (*n*=3) and 6 dptf (*n*=8). Scale bars: 100 μm in C–E; 20 μm in F; 50 μm in G. Significant differences are indicated. **P*<0.05, ***P*<0.01, ****P*<0.001, Mann–Whitney-test and *t*-test. Control indicates control mimic and antagonist (AR) cocktail; 7+25 indicates let-7 AR and miR-25 mimic cocktail; 7-25-124 indicates let-7 AR, miR-25 and miR-124 mimic cocktail. *n*, number of cultures of six to eight mice per culture.

cells, such that approximately one-third of the cells in each well expressed the reporter (Fig. 4B). These cultures were then transfected with the miR-25/let-7AR, miR-25/miR-124/let-7AR or control mimics/ARs.

The results for the Rlbp1-CreER:tdTomato MG were similar to those we obtained with the *Ascl1*:tdTomato cultures: treatment with

miR-25 and let-7-AR with or without miR-124 caused the Rlbp1-tdTomato⁺ cells to adopt a neuronal morphology, with small somata and fine branched processes (Fig. 4C,C',E,E'). Immunofluorescent labeling confirmed that the cells expressed neuronal genes, with ~30% of the miR-25/let-7AR-treated cells and 40% of the miR-25/let-7AR/miR-124-treated cells expressing TUJ1 (control: 2%,

Fig. 4H). In addition, ~40% of the miR-25/let-7AR and 50% of the miR-25/let-7AR/miR-124-treated MG expressed Otx2 6 days post-transfection, whereas only 7% of the cells in control wells expressed this marker (Fig. 4F,F',I). To further confirm that the neuronal cells arose from proliferating MG, we added EdU at the onset of the MG cultures (Fig. 4B), which results in labeling of all dividing MG. About 80% of all Rlbpl⁺TUJ⁺ were also EdU⁺, showing that these neurons originated from MG that underwent mitotic proliferation *in vitro* (Fig. 4G-G'',J). The presence of TUJ1⁺EdU⁺Rlbpl⁻ cells (Fig. 4G-G'', red arrow) is likely due to the fact that only one-third of the MG were treated with 4-hydroxytamoxifen and hence labeled with the reporter.

Taken together, these data indicate that miRNAs impact the ability of MG to generate neurons *in vitro*. To determine whether these treatments also affect MG proliferation, we added EdU after transfection (Fig. 5) to label S phase. We compared the cell numbers in the treated and control cultures. Six days after transfection we found a significant increase in Rlbpl:tdTomato⁺

cells for both cocktails (Fig. 5C-F) relative to controls, suggesting that the treatments increased the proliferation of the MG. EdU labeling confirmed that ~20% (miR-25/let-7AR) and 15% (miR-25/let-7AR/miR-124) of all Rlbpl:tdTomato had incorporated EdU, a significant increase over the control wells (Fig. 5G-J).

The experiments described above used MG isolated from the P11 mouse retinas. At this age, there are no progenitors remaining in the retina, but the MG still proliferate robustly in dissociated cell cultures (Pollak et al., 2013). The MG of older mice can be grown *in vitro* by using a feeder layer of young MG (Wohl et al., 2017) or if the adult MG are plated at high density (this study; Fig. 6). Using the latter method, we cultured MG of mice from 1-4 months of age and transfected them with the two miRNA cocktails (Fig. 6A,B). The MG from the mature mice responded to the miRNA cocktails much like the P11 cultures: there were Rlbpl:tdTomato⁺ cells that had small somata, fine processes and were TUJ1⁺ (Fig. 6C,C'-F', arrowheads). These were present as single,

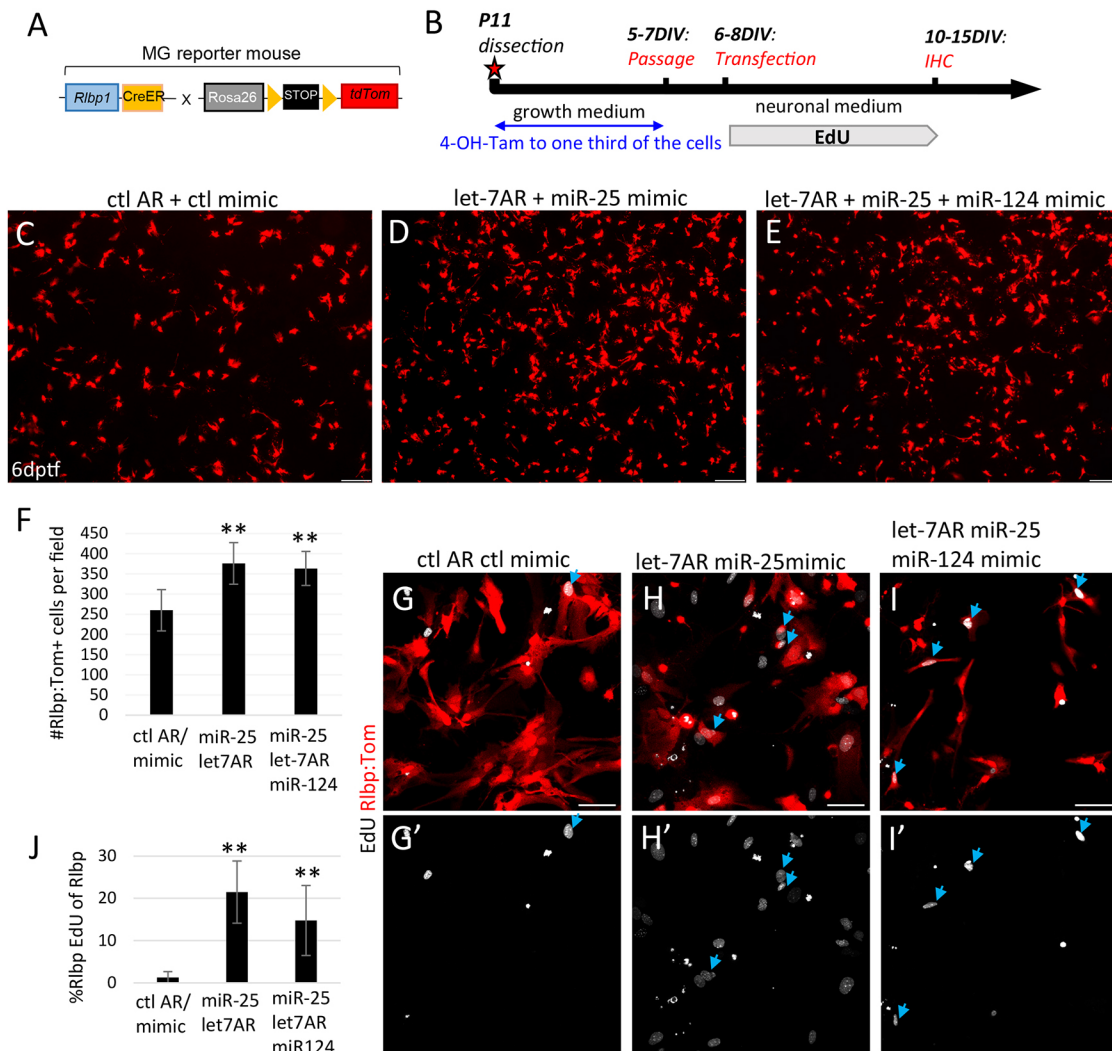


Fig. 5. miR-25/miR-124/let-7 reprogrammed Rlbpl⁺ MG increase in number due to proliferation. (A) Schematic of the *Rlbpl1*CreER: *tdTomato*^{flSTOP/STOP} construct. (B) Experimental design. (C-E) Live images of *tdTomato*⁺ cells after transfection with control, miR-25+let-7AR or miR-25+let-7AR+miR-124 at 6 days post transfection (dptf). (F) Number of Rlbpl:tdTomato⁺ cells per field in control and treatment groups ($n=6$). (G-I') Immunofluorescent labeling for *tdTomato* (Rlbpl) and EdU. Examples of cells positive for both markers are indicated by blue arrows. (J) Number of EdU⁺ Rlbpl:tdTomato⁺ cells per field at 3-5 dptf ($n=5$). Scale bars: 200 μ m in C-E; 50 μ m in G-I'. Significant differences are indicated. ** $P<0.01$, Mann-Whitney-test. n , number of cultures of six to eight mice per culture. ctl, control.

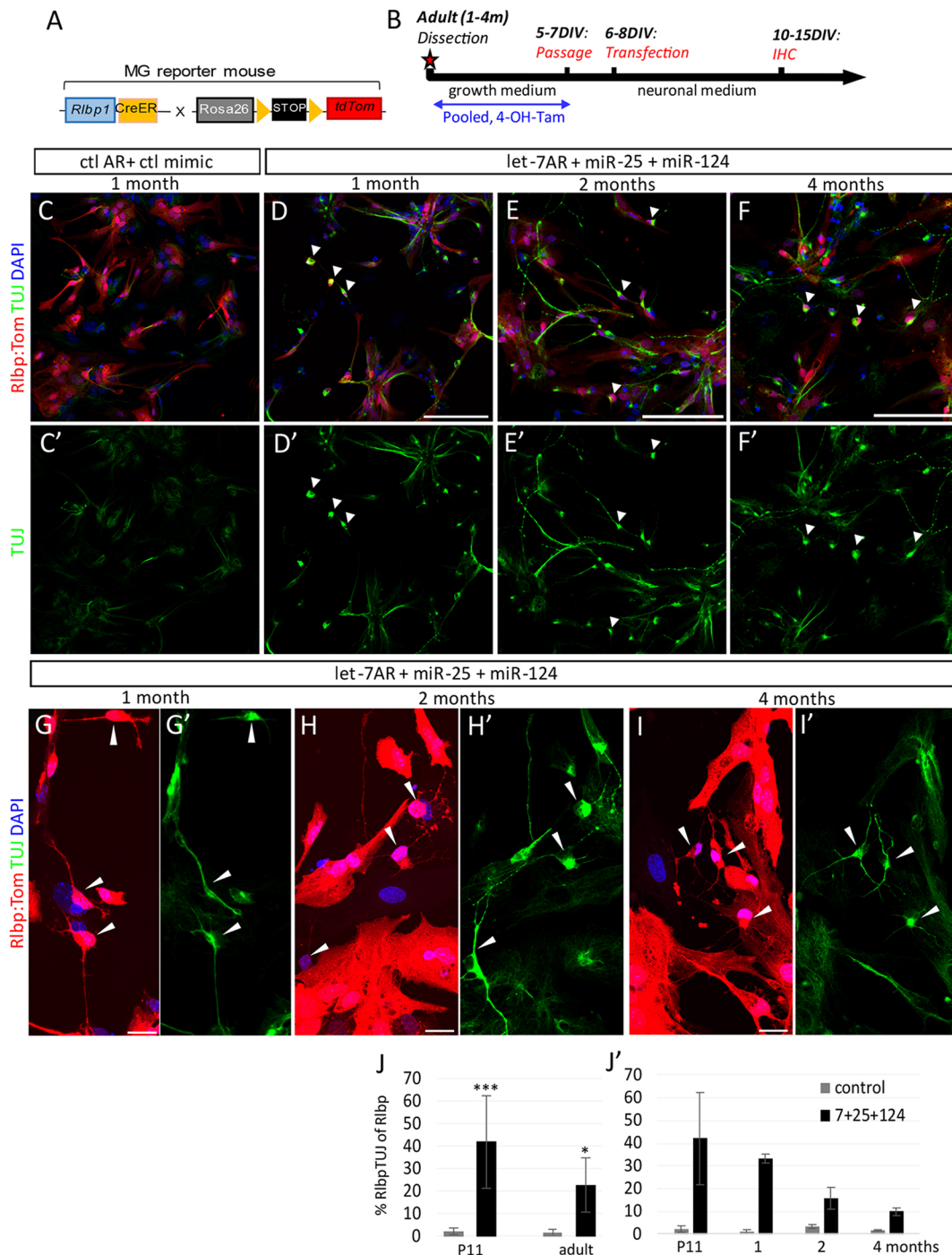


Fig. 6. miR-25/miR-124/let-7 can reprogram adult MG. (A) Schematic of the *Rlbp1*CreER: *tdTomato*^{flSTOP/STOP} construct. (B) Experimental design. (C-I') Immunofluorescent labeling for *tdTomato* (Rlbp1), TUJ1 and DAPI nuclear labeling of MG cultures from 1-, 2- and 4-month-old mice at 6 dptf. Examples for TUJ⁺ MG are indicated by arrowheads. Only cells with neuronal morphology were counted. (J) Graph showing the percentage of TUJ1⁺RlbpTom⁺ cells/total RlbpTom⁺ cells in cultures from P11 and adult mice (1-4 months pooled). (J') Percentage of TUJ1⁺Rlbp:tdTomato⁺ cells of total Rlbp:tdTomato⁺ cells from P11 (eight individual experiments), 1-month-old (two mice pooled, one experiment), 2-month-old (four mice pooled, one experiment) and 4-month-old mice (eight mice pooled, one experiment) at 6 dptf. Scale bars: 100 μ m in C-F'; 20 μ m in G-I'. Significant differences are indicated. *** P <0.001 (Mann-Whitney test).

isolated cells or in clusters of three to six cells, often associated with a flat MG (Fig. 6G/G'-I/I'). The potential of MG to convert into neuronal-like cells declines with age: in the P11 MG cultures, ~40% differentiate into neuron-like cells, while in the adult MG cultures (range 1-4 months), an average of 20% of the cells express TUJ1 after treatment with the miRNA reprogramming cocktail (Fig. 6J,J').

Single cell RNA-seq analysis of reprogrammed MG

To better characterize the mechanisms involved in the effects of miR-25 mimics and let-7 antagonism on MG fate, we carried out single cell RNA-seq (scRNA-seq). Cultured MG that had been transfected with either control mimics/ARs or one of four experimental groups (let-7AR, miR-25 mimic, miR-124 mimic, miR-25 and let-7AR or all three combined) were processed for

single cell analysis on the 10x Genomics platform. The cells were harvested 8 days after transfection and processed for single cell sequencing. The numbers of sequenced cells were 4874 (control), 5269 (miR-25), 5141 (miR-124), 3328 (let-7AR), 3933 (miR-25+let-7AR) and 3668 (miR-25+miR-124+let-7AR). After running the reads through the Cell Ranger pipeline, data were analyzed and normalized using the Seurat package. Linear dimensionality reduction was carried out using a principal component analysis (PCA), cells were clustered based on PCs and clusters visualized on tSNE plots.

In all wells, the cells were primarily MG, but other contaminating cell populations (e.g. microglia, endothelial cells and astrocytes) were also identified by their gene expression profiles (Fig. 7A,B, Fig. S5A-I). Most fibroblast-like cells were removed from further analysis, and the MG cells from control and treated cultures were combined to better characterize differences among the treatment conditions. In both control and treated conditions, most of the MG had a similar pattern of gene expression, although their differences allowed them to form several clusters. One cluster in particular had a retinal progenitor cell (RPC)-like gene expression profile and contained cells that expressed *Ascl1* and its downstream targets, such as *Hes6*, *Msi1* and *Dll1*. This cluster was primarily formed by cells that were treated with the combination of let-7AR with miR-25 and miR-124 mimics ('all', Fig. 7C-J). The induction of *Ascl1* and other progenitor genes in a subset of the MG by miR-25 mimics and let-7AR confirms the results with the *Ascl1* reporter (Fig. 2). This result further suggests that the decline in *Ascl1* during development, which accompanies the transition from RPCs to MG, is in part regulated by miRNAs. In addition to the progenitor-like cells, a smaller group of cells expressed more mature markers of retinal neuronal differentiation, including *Neurod1* (Fig. 7F), *doublecortin*, *Cabp5*, *Otx2*, *Neurod4*, *Grm6* and *Gap43* (growth cones; see Fig. 3F, arrows) as well as synaptic markers such as *synaptophysin* and *Snap25* (Fig. S6). The reprogrammed MG cluster was compared with previously published single cell RNA-seq data from FACS-sorted P17 bipolar cells, using either *Kncg4*-Cre or *Vsx2*-Cre to drive GFP using two different technologies (Shekhar et al., 2016). This analysis revealed that the reprogrammed glia have similar gene expression to normal bipolar cells (Fig. S7). Results from the scRNA-seq analysis extend the data from the immunofluorescence analyses and further support the idea that miRNAs can be used to reprogram MG to RPCs and neurons, similar to the overexpression of *Ascl1*.

To identify potential targets of miR-25, miR-124 and let-7 in MG, we compared each single treatment to the control cells using Seurat. We selected only the clusters that contained the MG, based on their expression of MG-specific genes. We then used 'Find Markers' in Seurat to select those genes that were most highly differentially expressed between MG in the treatment and the control conditions. We reasoned that those genes targeted by miR-25 or miR-124 would be reduced in the cells treated with these mimics, whereas the genes targeted by let-7 should show increases in the scRNA-seq data in the antagomiR-treated cells. For the cells treated with mimics for either miR-124 or miR-25, we selected those genes (top 100) with the greatest fold decreases, whereas for the let-7 antagomiR-treated cells, we selected those genes (top 100) that showed the greatest fold increase. These genes were then analyzed using the multiMiR package in Bioconductor to identify miRNA targets. The multiMiR package (Ru et al., 2014) allows retrieval of miRNA-target interactions from 14 external databases in R without the need to independently query these databases (~50 million interactions). The interactions were then be visualized with

igraph, a network visualization tool also implemented in R, by creating an adjacency matrix of miR:target interactions (igraph.org). The potential targets are shown as a graph, with the genes and miRNAs as the nodes in Fig. 8A.

Many of the potential targets of let-7, miR-25 and miR-124 are unique to each of these miRNAs. However, some of the genes that change the most in the scRNA-seq, such as transcription factor *Klf4* (Krüppel-like factor 4) and the Wnt antagonist *Dkk3* (Dickkopf 3), are targeted by two or three of these miRNAs (pink dots in Fig. 8A). Thus, some of the synergy observed in our experiments may stem from several miRNAs affecting the same target. Another key point is that targets of miR-124 that were identified in our analysis, *Tpm1* and *Itgb1* (Fig. 8A, yellow dots), have been previously identified as miR-124 targets in other cells (Hunt et al., 2011; Idichi et al., 2018; Neo et al., 2014). One gene in particular, *Ctdsp1* (Fig. 8B), a member of the Rest complex that has been previously reported to be a target of miR-124 (Nesti et al., 2014; Visvanathan et al., 2007), was identified in our earlier study of MG reprogramming with miR-124, and regulates *Ascl1* via the Rest pathway (Wohl and Reh, 2016b). It is therefore interesting that another of the top targets identified in this analysis is *Rcor1*, because this is also a member of the Rest complex that represses neural gene (Abrajano et al., 2009; Andres et al., 1999; Masserdotti et al., 2015; Qureshi et al., 2010). Some of the synergy between miR-25 and miR-124 in reprogramming MG to an RPC-like state may be due to Rest being potentially targeted by miR-25. Another target of miR-124, the cell cycle gene *cyclin D2* (*Ccnd2*) (Li et al., 2017), also showed a decline in expression in miR-124-treated MG (Fig. 8A, violin plot in C).

The gene targeted by let-7 (i.e. fold increase after let-7AR) was the transcription factor *Klf4* (Fig. 8D). *Klf4* is known to be expressed in MG and its expression increases after injury in chick and fish retina (Todd and Fischer, 2015; Todd et al., 2018; Zelinka et al., 2016). *Klf4* was among the first genes shown to promote reprogramming of fibroblasts to iPSCs (Gao et al., 2016; Hjelm et al., 2011; Wernig et al., 2008). Although this had not been previously shown to be a target of let-7, there are two predicted conserved let-7 sites in the 3'UTR of *Klf4* (Fig. 8E). Moreover, a recent study reported that let-7 inhibits reprogramming of human cells into iPSCs using the known reprogramming factors including *Klf4* (Worringer et al., 2014). Another gene that is expressed in MG and is known to be a target of let-7 in many cell types is that encoding the high motility group A2 protein (*Hmga2*) (Balzeau et al., 2017; Lee and Dutta, 2007; Patterson et al., 2014; Xia and Ahmad, 2016). There was a decline in levels of the Hmg family member *Hmgn2*, but not in *Hmga2* in the let-7AR-treated MG (Fig. 8F,G).

Other potential targets identified in our analysis have not been previously reported to be targets of these miRNAs. In terms of fold-change, the top target of miR-25 was *Dkk3*, a Wnt inhibitor (Fig. 8H). As activation of the Wnt pathway has previously been shown to stimulate MG proliferation (Das et al., 2006; Gallina et al., 2016; Nakamura et al., 2007; Ramachandran et al., 2011; Yao et al., 2016), the effect on *Dkk3* might in part explain the increase in MG proliferation we observe (Fig. 5). Moreover, an increase in Wnt signaling leads to activation of Wnt target genes such as the neuronal gene *Neurod1*, which was found in the scRNA-seq analysis (Fig. 7J). There are three predicted sites in the *Dkk3* 3'UTR (Fig. 8I); two studies report *Dkk3* is a direct target of miR-25 for other cell types (Huo et al., 2016; Yoshida et al., 2018) and two studies reporting that the miR-92 targets *Dkk3* in neural tissue (De Brouwer et al., 2012; Haug et al., 2011). miR-92 has the same seed sequence as miR-25 (Fig. S2A).

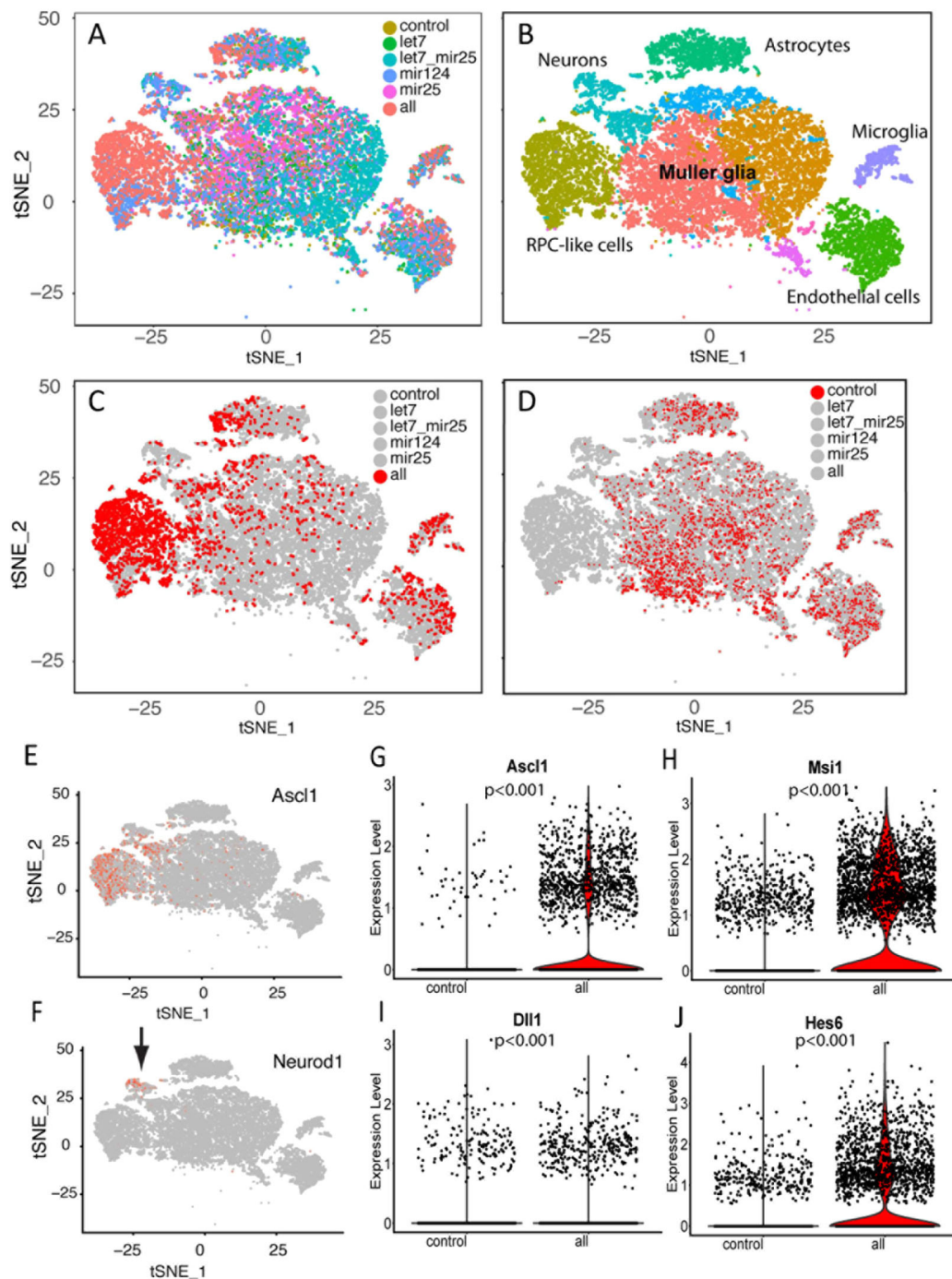


Fig. 7. Single cell RNA-seq of miRNA-mediated reprogramming of MG to RPCs and neurons. (A) Cells from all conditions were combined and clustered. tSNE plot shows the relative contributions to each cluster by treatment condition. (B) Clusters were designated as a specific cell type by the pattern of gene expression and known marker genes characteristic of that cell type. The largest cell cluster was made up of MG, but other cells, such as endothelial cells, microglia and astrocytes, were present as contaminating cell populations in the cultures. (C) Cells for the 'all' treatment condition (miR-25 and miR-124 mimics, with let-7 AR) are labeled red; the RPC-like cluster was largely made of cells that received this treatment. (D) Cells for the control condition are labeled red; these are not present in the 'neuron' cluster or the RPC-like cluster. (E) Cells expressing *Ascl1* are colored in red to show their distribution in the RPC-like cluster. (F) Cells expressing *Neurod1* are colored in red to show their distribution in the neuron cluster. (G–J) Violin plots to show the large increases in cell expressing progenitor genes in the 'all' (miR-25/124+let-7AR) treatment condition. Statistics for violin plots were calculated from gene expression on a per cell basis (unpaired two-tailed *t*-test). Significant differences are indicated ($P < 0.001$).

DISCUSSION

In this report, we have carried out an analysis in the differences in miRNA expression between RPCs and MG. The differences in miRNA expression coincide with differences in mRNA expression between the two cell types, and reflect the relationships among these

classes of molecules during the cell fate transition from RPCs to MG. One of the most important differences between RPCs and MG is their capacity for mitotic proliferation. RPCs are highly proliferative cells, whereas MG are quiescent in mice. Cell cycle genes are thus highly expressed in RPCs, but downregulated in the

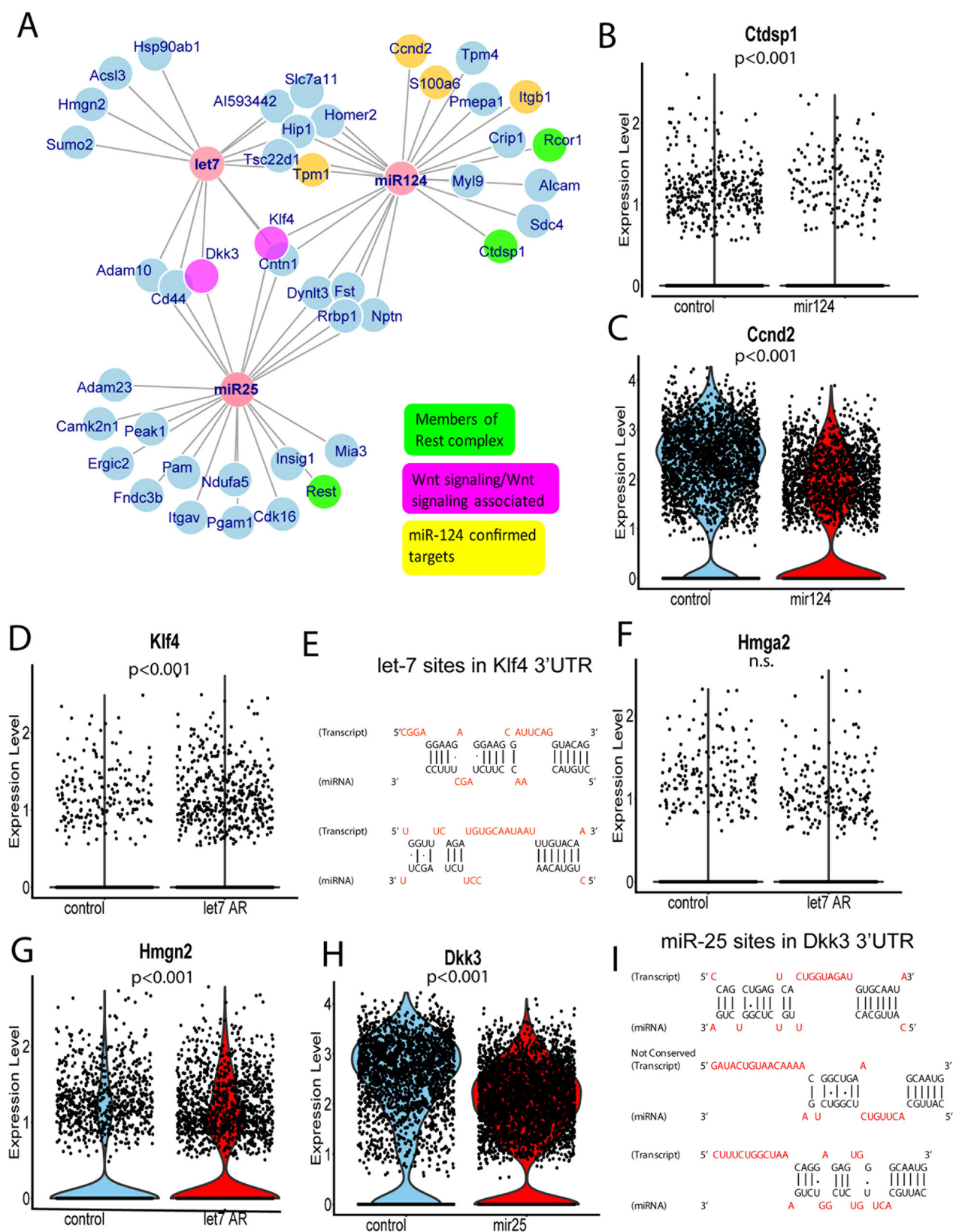


Fig. 8. See next page for legend.

MG (Nelson et al., 2011). Coincidentally, many miRNAs known to be important in cell cycle gene regulation are highly expressed in RPCs, but not in MG. Examples include miR-15a/b, miR-19a,

miR-17, miR-106 and miR-20a/b (summarized in Fig. 9). These are among the miRNAs that show the largest differences between the MG and RPCs, decline as the MG mature, and are

Fig. 8. Potential targets of reprogramming miRNAs in MG and RPCs.

(A) The single cell RNA-seq data were analyzed for significant changes across treatment groups using Seurat. The genes with reduced expression after the mimic treatment or with increased expression after let-7AR treatment were evaluated for the presence of predicted or known miRNA regulation. Gene-miRNA relationships are plotted as a graph with the nodes as either the genes (blue, green, pink or yellow) or miRNAs (coral). Genes shown in yellow are known targets of miR-124, genes shown in green are genes in the Rest pathway and genes in pink are those that change the most in the let-7AR or miR-25 conditions. (B,C) Violin plots of known targets of miR-124 showing the reduction in the number of cells expressing these genes in the miR-124-treated cells. (D-G) let-7 targets. (D,F,G,H) Violin plots of known targets of let-7 and miR-25. let-7 inhibition resulted in an increase in *Klf4* (D), but not *Hmga2* (F), expression. Although *Hmga2* expression is not altered in the let-7AR treated cells, a related factor, *Hmgn2*, is one of the most highly upregulated genes in cells treated with the let-7 antagonist (G). (H) *Dkk3*, a known target of miR-25 is decreased in miR-25 mimic-treated cells. (E,I) Predicted miRNA sites in *Dkk3* (I) and *Klf4* (E) from Diana Tools for let-7 (E) and miR-25 (I). (http://diana.imis.athena-innovation.gr/DianaTools/index.php?r=microT_CDS/results&keywords=ENSMUSG00000003032&genes=ENSMUSG00000003032%20&mirnas=&descr=&threshold=0.7 http://diana.imis.athena-innovation.gr/DianaTools/index.php?r=microT_CDS/results&keywords=ENSMUSG000000030772&genes=ENSMUSG000000030772%20&mirnas=&descr=&threshold=0.7 cell types). Statistics for violin plots were calculated on gene expression on a per cell basis (unpaired two-tailed *t*-test). Significant differences are indicated ($P < 0.001$).

well-established regulators of cyclins and cyclin-dependent kinases (Bueno and Malumbres, 2011). Some of the most highly expressed set of miRNAs in RPCs, those from the miR-106b-25 cluster (miR-106b, miR-92, miR-25), are products of the intron in the DNA replication licensing factor *Mcm7*, and so the levels of these miRNAs in RPCs might also be due to the much higher level of expression of *Mcm7* in RPCs than MG.

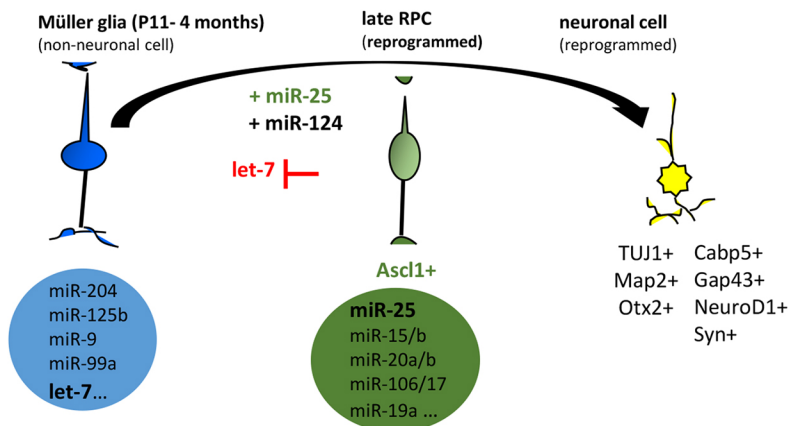
In addition to the changes in mitotic cell cycle that occur as RPCs differentiate into MG, there are also changes in the competence of the latter to generate neurons. Proneural genes, such as *Ascl1* and *Neurog2* are rapidly downregulated in the MG, along with other genes associated with neurogenesis, such as *musashi* (*Msi1*) and *nestin* (*Nes*). Previous studies in other areas of the nervous system have shown that miRNAs are critical regulators of neurogenesis and neurodevelopmental patterning. For example, miR-106 and miR-17 are necessary for the neurogenic-to-gliogenic transition in neural stem/progenitor cells from cerebral cortex: overexpression of miR-17 inhibits the acquisition of gliogenic competence by targeting p38/Mapk14 (Naka-Kaneda et al., 2014).

To better understand the roles of miRNAs in the processes of cell proliferation and neurogenesis in RPCs and MG, we manipulated

the expression of those that exhibited the greatest differences between these cells. Of the miRNAs we tested, we found the most significant effects with miR-25 and miR-124 mimics, and let-7 antagonists. As noted above, miR-25 is part of a cluster with miR-92 and miR-106b, in an intron in the *Mcm7* gene. A previous report demonstrated the importance of the miR-106b-25 cluster in primary cultures of neural stem progenitor cells, where knocking down miR-25 reduced neural stem/progenitor cell proliferation, whereas overexpression of the cluster increased neuron production (Brett et al., 2011). We find that miR-25 has similar effects on MG: increasing the levels of this miRNA with a specific mimic causes an increase in *Ascl1*⁺ MG-derived neuronal cells. Thus, miR-25 may have a more general role in maintaining the neural progenitor phenotype throughout the nervous system.

Another miRNA that was active in our reprogramming assay was let-7, a miRNA that has been already shown to be important for both neurogenesis and neural regeneration in previous reports. Originally identified as part of the heterochronic pathway in *C. elegans*, let-7 has important developmental roles in many tissues and organisms (Pasquinelli et al., 2000; Reinhart et al., 2000). The production of mature let-7 is regulated by Lin-28, another component of the heterochronic pathway in worms (Johnson et al., 2003; Reinhart et al., 2000) and one of the first genes identified as a reprogramming factor for generating iPSCs (Yu et al., 2007). In the embryonic mouse retina, let-7 and Lin-28 also have a crucial role in regulating developmental timing, specifically the transition of the RPCs from generating early fates to generating late cell identities (La Torre et al., 2013). A key step in retinal regeneration in zebrafish is the induction of Lin-28 by *Ascl1*. In this system, Lin-28 also inhibits let-7 maturation and this causes a further increase in *Ascl1* (Goldman, 2014; Ramachandran et al., 2010). Although we have not observed that *Ascl1* overexpression in MG can induce Lin-28 in mice, the second part of the feedback loop may be intact in mice, as let-7 inhibition leads to an *Ascl1* increase in mice (this study). Moreover, overexpression of Lin-28 in fish MG has been shown to stimulate their proliferation and expression of neural progenitor markers (Elsaedi et al., 2018; Ramachandran et al., 2010; Yao et al., 2016). In mice, Yao et al. reported that MG proliferation and the neurogenic potential of MG is regulated via Wnt signaling through a Lin-28/let-7-dependent pathway (Yao et al., 2016).

The third miRNA that we find reprograms MG to a more RPC-like state is miR-124. We previously reported that miR-124 could reprogram MG by targeting genes in the Rest pathway, including *Ctdsp1* and *Ptbp1* (Wohl and Reh, 2016b). In this study, we confirmed these findings using single cell RNA-seq, demonstrating

**Fig. 9. miR-25/124 and let-7 in MG reprogramming – suggested mechanisms.**

Identification of miRNAs highly expressed in mature Müller glia (MG; blue circle, top reprogramming candidate is let-7) and late retinal progenitor cells (RPCs; green circle, the top reprogramming candidate is miR-25). Overexpression of the RPC miRNA miR-25 with or without miR-124 (a miRNA known to reprogram MG into neurons) and antagonism of let-7 result in MG-derived progenitors, which differentiate into cells expressing neuronal markers (detected by immunohistochemistry and scRNA-seq).

that miR-124 causes increases in neural genes and neural progenitor genes, and a decrease in the expression of *Ctdsp1*. The relationship between miR-124 and the Rest pathway has been previously investigated in neural reprogramming in fibroblasts using miR-124 in combination with miR-9 and miR-9* that target different members of the Rest complex (Abernathy et al., 2017; Victor et al., 2014; Xue et al., 2013; Yoo et al., 2009, 2011). One of the mechanisms important for the miRNA-mediated conversion of fibroblasts to neurons involves the gene *Ptbp1*, an inhibitor of miR-124 (Makeyev et al., 2007; Xue et al., 2013). Recent evidence shows that the mechanisms of action of miR-124, miR9 and miR-9* also involves Usp14, Ezh2 and Rest (Lee et al., 2018). The level of Rest is regulated by a stabilizing methylation via the methyltransferase Ezh2, and the level of Ezh2 is in turn regulated by the deubiquitylating enzyme Usp14 (Doepfner et al., 2013; Lee et al., 2018). The miRNAs, miR-124 and miR-9 target Usp14, which leads to a decrease in Ezh2 levels, a loss of methylation of Rest and increased degradation of this neural gene repressor (Lee et al., 2018). The finding that ablation of Rest dramatically improves the efficiency of neural reprogramming in astrocytes (Masserdotti et al., 2015) indicates that some of these same mechanisms may be active in repressing neural genes in glia. In the MG, Usp14 was not one of the genes that changed significantly in the miR-124-treated cells, but Ezh2 deletion is known to have effects on retinal development (Zhang et al., 2015), including an early onset of neuron differentiation, consistent with a similar role in RPCs. Further studies will be needed to determine whether Ezh2 plays a role in retinal regeneration.

An interesting result from our study suggests miRNA-mediated regulation of Ascl1 levels in MG and possibly RPCs. Little is known about the regulation of Ascl1 expression or levels in RPCs. Our results in this paper and our previous report of miR-124 in MG reprogramming suggest that the Rest pathway is involved, either directly or indirectly, in the regulation of this key transcription factor. As our initial screen relied on changes in an Ascl1 reporter, it is not surprising that we find the miRNAs effective in this screen were those that induced increases in Ascl1 in the single cell RNA-seq, although the 3'UTR of Ascl1 does not appear to be targeted directly by these miRNAs. It is possible that miR-25 and let-7 also regulate Ascl1 levels via the Rest pathway, and there is a predicted site in miR-25 for Rest. However, it is also possible that other genes targeted by these miRNAs, such as *Dkk3* and *Klf4*, regulate Ascl1 expression. It is also worth noting that we only screened a subset of the most highly differentially expressed miRNAs in our assay, and it is likely that additional miRNAs are important in the maintenance of the cell state in the RPCs and MG; nevertheless, our results show that antagonizing let-7 and increasing levels of miR-25 and miR-124 using miRNA mimics is useful in reprogramming MG to retinal neurons *in vitro* and could help in stimulating regeneration in this system.

MATERIALS AND METHODS

Animals

All mice were housed at the University of Washington and all experiments were carried out in accordance with University of Washington Institutional Animal Care and Use Committee approved protocols (UW-IACUC). *Sox2-CreERT2* (017593) mice were obtained from Jackson Laboratories, *Ascl1-CreERT2* (012882) mice were a gift from Dr Jane Johnson (UT Southwestern Medical School, Dallas, TX, USA) and *Rlbp1-CreERT2* mice were obtained from Dr E. Levine at Vanderbilt University (Nashville, TN, USA) (Vázquez-Chona et al., 2009). All cre lines were crossed to *R26-stop-flox-CAG-tdTomato* mice (Jackson Laboratories, also known as Ai14 [007914]). Genotyping was carried out using the primers listed in Table S3. Tamoxifen (Sigma-Aldrich) was administered intraperitoneally at 75 mg/kg in corn oil at P0+1, P6+7, P9+10 for the P2, P8 and P11 analysis,

respectively, and for 2 consecutive days at ages $P>21$ for the adult assay. Males and females were used. Strains and ages are specified in every figure.

Fluorescence activated cell sorting (FACS)

Retinas of mice (P2, 4 mice; P8, 26 mice; P11, 16 mice; adult, 40 mice) were dissociated and confirmed for successful recombination under a fluorescence microscope (Zeiss Observer D1). For one sort, 6–10 retinas were pooled and dissociated in DNase/papain (75 μ l and 750 μ l, respectively, Worthington) for 20 min at 37°C on the shaker, triturated, mixed with ovomucoid (Worthington; 750 μ l) to stop the enzymatic reaction, centrifuged for 10 min at 300 *g* and resuspended in 600 μ l DNase/ovomucoid (Worthington)/Neurobasal (Gibco) (1:1:10) per retina. Cells were filtered through a 35 μ m filter to remove cell clumps, sorted using an 80 micron nozzle, and collected into two separate chilled tubes. Debris was excluded from the sort and only events in gate P1 were sorted (Fig. S1). Cells with the brightest fluorescence were found in gate P3 ['positives' (+), the RPC or MG fraction], while cells with no fluorescence were in gate P2 ['negatives' (–)], and everything in between was excluded. Post-sorts of the tdTomato⁺ RPC/MG were performed to assure high purification ($\geq 85\%$ tdTomato⁺ cells of total cells), which was validated as described previously (Wohl and Reh, 2016a). Samples were collected in bovine serum albumin (BSA)-coated tubes containing Neurobasal medium. Cell sorts were performed using a BD Aria III cell sorter (BD Bioscience). After collection, the tdTomato⁺ MG fractions were post-sorted to validate purity. In addition, one drop of each condition was plated on a coverslip and evaluated for purity. All other cells were spun for 10 min at 300 *g* at 4°C, the pellet was homogenized in Qiazol (Qiagen) and stored at –80°C.

Müller glia primary culture

Müller glia were dissociated (see above) from whole retinas of postnatal day (P) 11/12 mice and adult (1, 2 and 4 months) and grown in Neurobasal medium supplemented with N-2, tetracycline-free 10% fetal bovine serum (FBS, Clontech) and epidermal growth factor (EGF, R&D Systems, 100 ng/ml) as described previously (Ueki et al., 2012). After 5–7 days *in vitro* (DIV), cells were either passaged on six-well or poly-ornithine (Poly-O, Sigma-Aldrich) and laminin (Gibco, Life Science Corporation) coated coverslips in 24-well plates. For the AsclCreER (RPC) reporter mouse, 4-hydroxytamoxifen was added after miRNA transfection (the time point of cre induction) until fixation/termination. Adding 4-hydroxytamoxifen from the beginning of the cultures did not result in prominent tdTomato expression. For the young (P11) Rlbp1CreER (MG) reporter mouse, 4-hydroxytamoxifen was added from the beginning of the culture until passage, to label MG. As all MG express Rlbp1, we labeled only one-third of the cells to allow cell tracking and cell characterization. After passage, we combined labeled with unlabeled MG. For the adult Rlbp1Cre-reporter cultures, 4-hydroxytamoxifen was added to the pooled tissue until passage. EdU was added either with the onset of culturing to track cell proliferation of MG lineage or after transfection to quantify cell proliferation due to the treatment. Cultures that did not display good cell growth and did not become confluent were excluded from further processing.

Transfection

We carried out RNA transfection with miRNA mimics and/or antagomiRs (Table S4, Thermo Fisher Scientific) as follows: for individual mimics or antagomiR, the final concentration in the medium was 500 nM; in the case where multiple mimics were added, or combined with an antagomiR, each RNA was present in the medium at a final concentration of 500 nM. MG cultures from Ascl1-CreER:tdTomato or Rlbp1-CreER:tdTomato mice were transfected using Lipofectamine 3000 in Optimem medium, in accordance with the manufacturer's instructions. Three hours after transfection, the medium was changed to either normal medium [1% FBS with B27 supplement and BDNF (100 ng/ml)] or BrainPhys neuronal medium (Stemcell Technologies) supplemented with B27, N2, BDNF (20 ng/ml), GDNF (20 μ g/ml), dibutyl-*c*-AMP (1 mM) and ascorbic acid (200 nM, see Bardy et al., 2015).

RNA purification and miRNA profiling

The sorts of all retinas per age were pooled for the RNA purification (P2, 4 mice; P8, 26 mice; P11, 16 mice; adult, 40 mice). RNA was extracted and

purified with a miRNeasy Micro Kit in accordance with the manufacturer's instructions (Qiagen). NanoString nCounter software was used for miRNA expression analysis. DNA sequences called miRtags were ligated to the mature miRNAs through complementary oligonucleotides with sequence-specific binding (bridges). All excess tags and bridges were removed, resulting in sequence-specific tagging of mature miRNAs. The miRtagged mature miRNA was then hybridized to a probe pair (reporter probe with a barcode and capture probe complementary to the miRNA) in the standard nCounter gene expression array workflow. 200 ng of total RNA per sample (33 ng/ μ l per sample) was submitted for NanoString analysis, performed at the Fred Hutchinson Cancer Center (Seattle, WA, USA). NanoString data were analyzed using nSolver 2.6 software. The data represent counts of molecules normalized against four housekeeping genes (β -actin, *Gapdh*, *Rpl19* and *B2m*), eight negative controls and six positive controls that were run simultaneously with the samples.

Single cell RNA-sequencing (scRNA-seq)

Cultures of MG (2 \times 8 pooled mice) were dissociated from the plate and cells were pelleted at 300 g for 10 min at 4°C. Cells were then suspended in 0.04% BSA in PBS at a concentration of 2000 cells per μ l and loaded onto the Single Cell 3' Chip (10x Genomics) with a targeted cell recovery of 4000 cells. GEM generation and barcoding, RT, cleanup, cDNA amplification and library construction were performed according to the manufacturer's instructions. Single cell libraries were sequenced with the Illumina NextSeq 500/550 v2 kit. Reads were processed in Cell Ranger (10x Genomics), aligned to Mm10 and analyzed in Seurat using R-software. Data were analyzed and normalized by the percentage of mitochondrial genes and the number of genes per cell. The data were then scaled (by total expression) and log transformed. The scaled z-scores from Seurat's ScaleData function were used for dimensionality reduction and clustering. Linear dimensionality reduction was carried out using a principal components analysis (PCA) and the PCA scores are used for clustering. Non-linear dimensional reduction (tSNE) was used to visualize the cell clusters and explore components of the data. Differentially expressed genes were found using the default Wilcoxon rank sum test. Analysis of miRNA targets was carried out using the Bioconductor package multiMIR (Ru et al., 2014), and the interactions were visualized with igraph (igraph.org). Predicted miRNA target sites in specified genes were identified using Diana Tools microT-CDS (Paraskevopoulou et al., 2013; Reczko et al., 2012) (diana.imis.athena-innovation.gr/DianaTools). Single cell RNA seq data from MG progenitor and reprogrammed clusters were integrated with existing retinal datasets using the Integrate data functions in Seurat version 3, which uses identification of mutual nearest neighbors and canonical correlation analysis (CCA) to integrate datasets and remove batch effects (Stuart et al., 2019). Unpaired, two-tailed *t*-test was used to compare the expression levels of miRNA-treated MG with control on gene expression on a per cell basis. Differences were considered to be statistically significant if $P < 0.05$.

Fixation, sectioning and immunofluorescent labeling

MG cultures were fixed with 2% PFA. For immunofluorescent staining, cells were incubated in blocking solution (5% milk block: 2.5 g non-fat milk powder in 50 ml PBS; with 0.5% Triton-X100) for 1 h at room temperature. Primary antibodies (Table S5) were incubated in 5% milk block overnight, secondary antibodies (Table S6) were incubated for 1 h at room temperature and counterstained with 4,6-diamidino-2-phenylindole (DAPI, Sigma-Aldrich, 1:1000). EdU labeling was carried out using Click-iT EdU Kit (Invitrogen).

Microscopy, cell counts and statistical analysis

Live imaging was performed using Zeiss Observer D1 with Axio-Cam. The number of living cells per field were evaluated for five random fields per coverslip, at 50 \times magnification using ImageJ. Live images were evaluated blinded. Fixed cells were analyzed by LSM880 confocal microscope and ZEN software (Zeiss, Germany). Three to five random fields per coverslip, at 200 \times magnification were counted and averaged for every condition. For high-power images, pictures were taken at 600 \times magnification. Values are expressed as mean \pm s.d. The sample size was based on our previous studies

showing adequate power. For cell cultures, six to eight mice were pooled for one experiment, *n* given in the figures represents the number of cultures (experiments). Statistical analyses were performed using Shapiro-Wilk to test for normal distribution followed by either a Mann-Whitney test {non-parametric, exact significance [$2 \times (1 - \text{tailed})$] } or a two-tailed *t*-test for independent samples combined with Levene's test for equality of variances, using SPSS software. Holm-Bonferroni method was used to correct for multiple comparisons. Images were processed and assembled using Adobe Photoshop and Adobe Illustrator.

Acknowledgements

The authors thank Donna Prunkard and Jeanne Fredrickson from the Department of Pathology for assistance with the FAC-sorter, Alex Chitsazan for bioinformatic analyses assistance, Dr Akshaya Sridhar for providing the neuronal differentiation protocol, and Andy Shimchuk, Ian Mount and Ellen Bercaw for lab assistance. The authors thank Dr Olivia Bermingham-McDonogh and all members of the Reh lab for helpful comments on the manuscript, and for their critical input during the course of this work. We thank The Vision Core (P30EY01730) for the use of their imaging facilities.

Competing interests

The authors declare no competing or financial interests.

Author contributions

Conceptualization: S.G.W., T.A.R.; Methodology: S.G.W., M.J.H.; Software: M.J.H.; Validation: S.G.W., M.J.H.; Formal analysis: S.G.W., M.J.H., T.A.R.; Investigation: S.G.W.; Resources: T.A.R.; Data curation: S.G.W., T.A.R.; Writing - original draft: S.G.W., T.A.R.; Writing - review & editing: S.G.W., M.J.H., T.A.R.; Visualization: S.G.W., T.A.R.; Funding acquisition: T.A.R.

Funding

Grants and financial support provided by the National Eye Institute (NEI R01EY021482 to T.A.R.), by the Deutsche Forschungsgemeinschaft (Wo 2010/1-1), by The State University of New York Empire Innovation Program (1706 to S.G.W.) and by the Foundation Fighting Blindness (TA-RM-0614-0650-UWA to T.A.R.). T.A.R. also acknowledges support from the Paul G. Allen Family Foundation Distinguished Investigator fund. Deposited in PMC for release after 12 months.

Data availability

Nanostring (GSE135835) and sc-RNA-seq (GSE135816) data have been deposited in GEO under SuperSeries accession number GSE135846.

Supplementary information

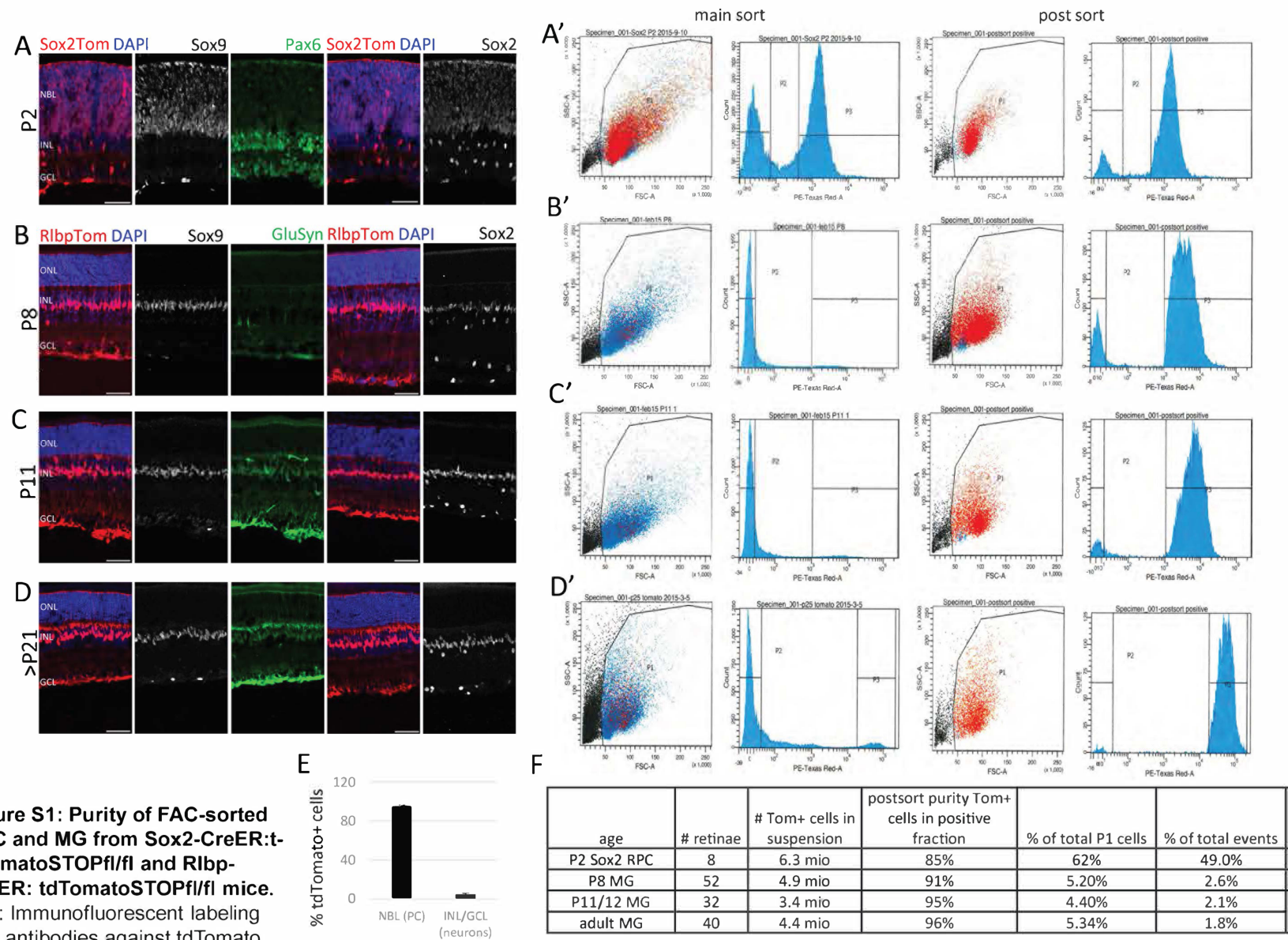
Supplementary information available online at <http://dev.biologists.org/lookup/doi/10.1242/dev.179556.supplemental>

References

- Abernathy, D. G., Kim, W. K., McCoy, M. J., Lake, A. M., Ouwenga, R., Lee, S. W., Xing, X., Li, D., Lee, H. J., Heuckeroth, R. O. et al. (2017). MicroRNAs induce a permissive chromatin environment that enables neuronal subtype-specific reprogramming of adult human fibroblasts. *Cell Stem Cell* **21**, 332-348.e339. doi:10.1016/j.stem.2017.08.002
- Abrajano, J. J., Qureshi, I. A., Gokhan, S., Zheng, D., Bergman, A. and Mehler, M. F. (2009). REST and CoREST modulate neuronal subtype specification, maturation and maintenance. *PLoS ONE* **4**, e7936. doi:10.1371/journal.pone.0007936
- Andres, M. E., Burger, C., Peral-Rubio, M. J., Battaglioli, E., Anderson, M. E., Grimes, J., Dallman, J., Ballas, N. and Mandel, G. (1999). CoREST: a functional corepressor required for regulation of neural-specific gene expression. *Proc. Natl. Acad. Sci. USA* **96**, 9873-9878. doi:10.1073/pnas.96.17.9873
- Balzeau, J., Menezes, M. R., Cao, S. and Hagan, J. P. (2017). The LIN28/let-7 pathway in cancer. *Front. Genet.* **8**, 31. doi:10.3389/fgene.2017.00031
- Bardy, C., van den Hurk, M., Eames, T., Marchand, C., Hernandez, R. V., Kellogg, M., Gorris, B., Galet, B., Palomares, V., Brown, J. et al. (2015). Neuronal medium that supports basic synaptic functions and activity of human neurons in vitro. *Proc. Natl. Acad. Sci. USA* **112**, E2725-E2734. doi:10.1073/pnas.1504393112
- Beveridge, N. J., Tooney, P. A., Carroll, A. P., Tran, N. and Cairns, M. J. (2009). Down-regulation of miR-17 family expression in response to retinoic acid induced neuronal differentiation. *Cell. Signal.* **21**, 1837-1845. doi:10.1016/j.cellsig.2009.07.019
- Blackshaw, S., Harpavat, S., Trimarchi, J., Cai, L., Huang, H., Kuo, W. P., Weber, G., Lee, K., Fraioli, R. E., Cho, S.-H. et al. (2004). Genomic analysis of mouse retinal development. *PLoS Biol.* **2**, e247. doi:10.1371/journal.pbio.0020247

- Brett, J. O., Renault, V. M., Rafalski, V. A., Webb, A. E. and Brunet, A. (2011). The microRNA cluster miR-106b~25 regulates adult neural stem/progenitor cell proliferation and neuronal differentiation. *Aging* **3**, 108–124. doi:10.18632/aging.100285
- Brzezinski, J. A., IV, Kim, E. J., Johnson, J. E. and Reh, T. A. (2011). Ascl1 expression defines a subpopulation of lineage-restricted progenitors in the mammalian retina. *Development* **138**, 3519–3531. doi:10.1242/dev.064006
- Bueno, M. J. and Malumbres, M. (2011). MicroRNAs and the cell cycle. *Biochim. Biophys. Acta* **1812**, 592–601. doi:10.1016/j.bbdis.2011.02.002
- Busskamp, V., Krol, J., Nelidova, D., Daum, J., Szikra, T., Tsuda, B., Jüttner, J., Farrow, K., Scherf, B. G., Alvarez, C. P. P. et al. (2014). miRNAs 182 and 183 are necessary to maintain adult cone photoreceptor outer segments and visual function. *Neuron* **83**, 586–600. doi:10.1016/j.neuron.2014.06.020
- Das, A. V., Mallya, K. B., Zhao, X., Ahmad, F., Bhattacharya, S., Thoreson, W. B., Hegde, G. V. and Ahmad, I. (2006). Neural stem cell properties of Müller glia in the mammalian retina: regulation by Notch and Wnt signaling. *Dev. Biol.* **299**, 283–302. doi:10.1016/j.ydbio.2006.07.029
- De Brouwer, S., Mestdag, P., Lambertz, I., Pattyn, F., De Paepe, A., Westermann, F., Schroeder, C., Schulte, J. H., Schramm, A., De Preter, K. et al. (2012). Dickkopf-3 is regulated by the MYCN-induced miR-17-92 cluster in neuroblastoma. *Int. J. Cancer* **130**, 2591–2598. doi:10.1002/ijc.26295
- Dennis, L., Rhodes, M. and Maclean, K. (2015). Targeted miRNA discovery and validation using the nCounter® platform. WHITE PAPER NanoString Technologies 1.0.
- Doepfner, T. R., Doehring, M., Bretschneider, E., Zechariah, A., Kaltwasser, B., Müller, B., Koch, J. C., Bähr, M., Hermann, D. M. and Michel, U. (2013). MicroRNA-124 protects against focal cerebral ischemia via mechanisms involving Usp14-dependent REST degradation. *Acta Neuropathol.* **126**, 251–265. doi:10.1007/s00401-013-1142-5
- Elsaiedi, F., Macpherson, P., Mills, E. A., Jui, J., Flannery, J. G. and Goldman, D. (2018). Notch suppression collaborates with Ascl1 and Lin28 to unleash a regenerative response in fish retina, but not in mice. *J. Neurosci.* **38**, 2246–2261. doi:10.1523/JNEUROSCI.2126-17.2018
- Foshay, K. M. and Gallicano, G. I. (2009). miR-17 family miRNAs are expressed during early mammalian development and regulate stem cell differentiation. *Dev. Biol.* **326**, 431–443. doi:10.1016/j.ydbio.2008.11.016
- Gallina, D., Palazzo, I., Steffenson, L., Todd, L. and Fischer, A. J. (2016). Wnt/ beta-catenin-signaling and the formation of Müller glia-derived progenitors in the chick retina. *Dev. Neurobiol.* **76**, 983–1002. doi:10.1002/dneu.22370
- Gao, X., Wang, X., Xiong, W. and Chen, J. (2016). In vivo reprogramming reactive glia into iPSCs to produce new neurons in the cortex following traumatic brain injury. *Sci. Rep.* **6**, 22490. doi:10.1038/srep22490
- Geiss, G. K., Bumgarner, R. E., Birditt, B., Dahl, T., Dowidar, N., Dunaway, D. L., Fell, H. P., Ferree, S., George, R. D., Grogan, T. et al. (2008). Direct multiplexed measurement of gene expression with color-coded probe pairs. *Nat. Biotechnol.* **26**, 317–325. doi:10.1038/nbt1385
- Goldman, D. (2014). Müller glial cell reprogramming and retina regeneration. *Nat. Rev. Neurosci.* **15**, 431–442. doi:10.1038/nrn3723
- Grosche, A., Hauser, A., Lepper, M. F., Mayo, R., von Toerne, C., Merl-Pham, J. and Hauck, S. M. (2016). The proteome of native adult Müller glial cells from murine retina. *Mol. Cell. Proteomics* **15**, 462–480. doi:10.1074/mcp.M115.052183
- Haug, B. H., Henriksen, J. R., Buechner, J., Geerts, D., Tømte, E., Kogner, P., Martinsson, T., Flægstad, T., Sveinbjørnsson, B. and Einvik, C. (2011). MYCN-regulated miRNA-92 inhibits secretion of the tumor suppressor DICKKOPF-3 (DKK3) in neuroblastoma. *Carcinogenesis* **32**, 1005–1012. doi:10.1093/carcin/bgr073
- Hjelm, B. E., Rosenberg, J. B., Szelinger, S., Sue, L. I., Beach, T. G., Huentelman, M. J. and Craig, D. W. (2011). Induction of pluripotent stem cells from autopsy donor-derived somatic cells. *Neurosci. Lett.* **502**, 219–224. doi:10.1016/j.neulet.2011.07.048
- Hunt, S., Jones, A. V., Hinsley, E. E., Whawell, S. A. and Lambert, D. W. (2011). MicroRNA-124 suppresses oral squamous cell carcinoma motility by targeting ITGB1. *FEBS Lett.* **585**, 187–192. doi:10.1016/j.febslet.2010.11.038
- Huo, J., Zhang, Y., Li, R., Wang, Y., Wu, J. and Zhang, D. (2016). Upregulated microRNA-25 mediates the migration of melanoma cells by targeting DKK3 through the WNT/beta-catenin pathway. *Int. J. Mol. Sci.* **17**, 1124. doi:10.3390/ijms17111124
- Idichi, T., Seki, N., Kurahara, H., Fukuhisa, H., Toda, H., Shimonosono, M., Yamada, Y., Arai, T., Kita, Y., Kijima, Y. et al. (2018). Involvement of anti-tumor miR-124-3p and its targets in the pathogenesis of pancreatic ductal adenocarcinoma: direct regulation of ITGA3 and ITGB1 by miR-124-3p. *Oncotarget* **9**, 28849–28865. doi:10.18632/oncotarget.25599
- Jadhav, A. P., Roesch, K. and Cepko, C. L. (2009). Development and neurogenic potential of Müller glial cells in the vertebrate retina. *Prog. Retin. Eye Res.* **28**, 249–262. doi:10.1016/j.preteyeres.2009.05.002
- Jeon, C.-J., Strettoi, E. and Masland, R. H. (1998). The major cell populations of the mouse retina. *J. Neurosci.* **18**, 8936–8946. doi:10.1523/JNEUROSCI.18-21-08936.1998
- Jin, J., Kim, S.-N., Liu, X., Zhang, H., Zhang, C., Seo, J.-S., Kim, Y. and Sun, T. (2016). miR-17-92 cluster regulates adult hippocampal neurogenesis, anxiety, and depression. *Cell Rep.* **16**, 1653–1663. doi:10.1016/j.celrep.2016.06.101
- Jin, J., Ko, H., Sun, T. and Kim, S.-N. (2018). Distinct function of miR-17-92 cluster in the dorsal and ventral adult hippocampal neurogenesis. *Biochem. Biophys. Res. Commun.* **503**, 1594–1598. doi:10.1016/j.bbrc.2018.07.086
- Johnson, S. M., Lin, S.-Y. and Slack, F. J. (2003). The time of appearance of the *C. elegans* let-7 microRNA is transcriptionally controlled utilizing a temporal regulatory element in its promoter. *Dev. Biol.* **259**, 364–379. doi:10.1016/S0012-1606(03)00202-1
- Jorstad, N. L., Wilken, M. S., Grimes, W. N., Wohl, S. G., VandenBosch, L. S., Yoshimatsu, T., Wong, R. O., Rieke, F. and Reh, T. A. (2017). Stimulation of functional neuronal regeneration from Müller glia in adult mice. *Nature* **548**, 103–107. doi:10.1038/nature23283
- Karl, M. O., Hayes, S., Nelson, B. R., Tan, K., Buckingham, B. and Reh, T. A. (2008). Stimulation of neural regeneration in the mouse retina. *Proc. Natl. Acad. Sci. U.S.A.* **105**, 19508–19513. doi:10.1073/pnas.0807453105
- Karl, M. O. and Reh, T. A. (2010). Regenerative medicine for retinal diseases: activating endogenous repair mechanisms. *Trends Mol. Med.* **16**, 193–202. doi:10.1016/j.molmed.2010.02.003
- La Torre, A., Georgi, S. and Reh, T. A. (2013). Conserved microRNA pathway regulates developmental timing of retinal neurogenesis. *Proc. Natl. Acad. Sci. USA* **110**, E2362–E2370. doi:10.1073/pnas.1301837110
- Lee, Y. S. and Dutta, A. (2007). The tumor suppressor microRNA let-7 represses the HMGA2 oncogene. *Genes Dev.* **21**, 1025–1030. doi:10.1101/gad.154047
- Lee, S. W., Oh, Y. M., Lu, Y.-L., Kim, W. K. and Yoo, A. S. (2018). MicroRNAs overcome cell fate barrier by reducing EZH2-controlled REST stability during neuronal conversion of human adult fibroblasts. *Dev. Cell* **46**, 73–84.e77. doi:10.1016/j.devcel.2018.06.007
- Li, Y., Shao, G., Zhang, M., Zhu, F., Zhao, B., He, C. and Zhang, Z. (2017). miR-124 represses the mesenchymal features and suppresses metastasis in Ewing sarcoma. *Oncotarget* **8**, 10274–10286. doi:10.18632/oncotarget.14394
- Löffler, K., Schäfer, P., Völkner, M., Holdt, T. and Karl, M. O. (2015). Age-dependent Müller glia neurogenic competence in the mouse retina. *Glia* **63**, 1809–1824. doi:10.1002/glia.22846
- Makeyev, E. V., Zhang, J., Carrasco, M. A. and Maniatis, T. (2007). The MicroRNA miR-124 promotes neuronal differentiation by triggering brain-specific alternative pre-mRNA splicing. *Mol. Cell* **27**, 435–448. doi:10.1016/j.molcel.2007.07.015
- Mao, S., Li, H., Sun, Q., Zen, K., Zhang, C.-Y. and Li, L. (2014). miR-17 regulates the proliferation and differentiation of the neural precursor cells during mouse corticogenesis. *FEBS J.* **281**, 1144–1158. doi:10.1111/febs.12680
- Masserdotti, G., Gillotin, S., Sutor, B., Drechsel, D., Irmeler, M., Jørgensen, H. F., Sass, S., Theis, F. J., Beckers, J., Berninger, B. et al. (2015). Transcriptional mechanisms of proneural factors and REST in regulating neuronal reprogramming of astrocytes. *Cell Stem Cell* **17**, 74–88. doi:10.1016/j.stem.2015.05.014
- Naka-Kaneda, H., Nakamura, S., Igarashi, M., Aoi, H., Kanki, H., Tsuyama, J., Tsutsumi, S., Aburatani, H., Shimazaki, T. and Okano, H. (2014). The miR-17/106-p38 axis is a key regulator of the neurogenic-to-gliogenic transition in developing neural stem/progenitor cells. *Proc. Natl. Acad. Sci. USA* **111**, 1604–1609. doi:10.1073/pnas.1315567111
- Nakamura, R. E. I., Hunter, D. D., Yi, H., Brunken, W. J. and Hackam, A. S. (2007). Identification of two novel activities of the Wnt signaling regulator Dickkopf 3 and characterization of its expression in the mouse retina. *BMC Cell Biol.* **8**, 52. doi:10.1186/1471-2121-8-52
- Nelson, B. R., Ueki, Y., Reardon, S., Karl, M. O., Georgi, S., Hartman, B. H., Lamba, D. A. and Reh, T. A. (2011). Genome-wide analysis of Müller glial differentiation reveals a requirement for Notch signaling in postmitotic cells to maintain the glial fate. *PLoS ONE* **6**, e22817. doi:10.1371/journal.pone.0022817
- Neo, W. H., Yap, K., Lee, S. H., Looi, L. S., Khandelia, P., Neo, S. X., Makeyev, E. V. and Su, I.-H. (2014). MicroRNA miR-124 controls the choice between neuronal and astrocyte differentiation by fine-tuning *Ezh2* expression. *J. Biol. Chem.* **289**, 20788–20801. doi:10.1074/jbc.M113.525493
- Nesti, E., Corson, G. M., McCleskey, M., Oyer, J. A. and Mandel, G. (2014). C-terminal domain small phosphatase 1 and MAP kinase reciprocally control REST stability and neuronal differentiation. *Proc. Natl. Acad. Sci. USA* **111**, E3929–E3936. doi:10.1073/pnas.1414770111
- Paraskevopoulou, M. D., Georgakilas, G., Kostoulas, N., Reczko, M., Maragkakis, M., Dalamagas, T. M. and Hatzigeorgiou, A. G. (2013). DIANA-LncBase: experimentally verified and computationally predicted microRNA targets on long non-coding RNAs. *Nucleic Acids Res.* **41**, D239–D245. doi:10.1093/nar/gks1246
- Pasquinelli, A. E., Reinhart, B. J., Slack, F., Martindale, M. Q., Kuroda, M. I., Maller, B., Hayward, D. C., Ball, E. E., Degan, B., Müller, P. et al. (2000). Conservation of the sequence and temporal expression of let-7 heterochronic regulatory RNA. *Nature* **408**, 86–89. doi:10.1038/35040556
- Patterson, M., Gaeta, X., Loo, K., Edwards, M., Smale, S., Cinkornpumin, J., Xie, Y., Listgarten, J., Azghadi, S., Douglass, S. M. et al. (2014). let-7 miRNAs can act through notch to regulate human gliogenesis. *Stem Cell Rep.* **3**, 758–773. doi:10.1016/j.stemcr.2014.08.015

- Pollak, J., Wilken, M. S., Ueki, Y., Cox, K. E., Sullivan, J. M., Taylor, R. J., Levine, E. M. and Reh, T. A. (2013). ASCL1 reprograms mouse Müller glia into neurogenic retinal progenitors. *Development* **140**, 2619-2631. doi:10.1242/dev.091355
- Qureshi, I. A., Gokhan, S. and Mehler, M. F. (2010). REST and CoREST are transcriptional and epigenetic regulators of seminal neural fate decisions. *Cell Cycle* **9**, 4477-4486. doi:10.4161/cc.9.22.13973
- Rajaram, K., Harding, R. L., Bailey, T., Patton, J. G. and Hyde, D. R. (2014). Dynamic miRNA expression patterns during retinal regeneration in zebrafish: reduced dicer or miRNA expression suppresses proliferation of Müller glia-derived neuronal progenitor cells. *Dev. Dyn.* **243**, 1591-1605. doi:10.1002/dvdy.24188
- Ramachandran, R., Fausett, B. V. and Goldman, D. (2010). Ascl1a regulates Müller glia dedifferentiation and retinal regeneration through a Lin-28-dependent, let-7 microRNA signalling pathway. *Nat. Cell Biol.* **12**, 1101-1107. doi:10.1038/ncb2115
- Ramachandran, R., Zhao, X.-F. and Goldman, D. (2011). Ascl1a/Dkk/beta-catenin signaling pathway is necessary and glycogen synthase kinase-3beta inhibition is sufficient for zebrafish retina regeneration. *Proc. Natl. Acad. Sci. USA* **108**, 15858-15863. doi:10.1073/pnas.1107220108
- Reczek, M., Maragkakis, M., Alexiou, P., Grosse, I. and Hatzigeorgiou, A. G. (2012). Functional microRNA targets in protein coding sequences. *Bioinformatics* **28**, 771-776. doi:10.1093/bioinformatics/bts043
- Reinhart, B. J., Slack, F. J., Basson, M., Pasquinelli, A. E., Bettinger, J. C., Rougvie, A. E., Horvitz, H. R. and Ruvkun, G. (2000). The 21-nucleotide let-7 RNA regulates developmental timing in *Caenorhabditis elegans*. *Nature* **403**, 901-906. doi:10.1038/35002607
- Roesch, K., Jadhav, A. P., Trimarchi, J. M., Stadler, M. B., Roska, B., Sun, B. B. and Cepko, C. L. (2008). The transcriptome of retinal Müller glial cells. *J. Comp. Neurol.* **509**, 225-238. doi:10.1002/cne.21730
- Ru, Y., Kechris, K. J., Tabakoff, B., Hoffman, P., Radcliffe, R. A., Bowler, R., Mahaffey, S., Rossi, S., Calin, G. A., Bemis, L. et al. (2014). The multiMIR R package and database: integration of microRNA-target interactions along with their disease and drug associations. *Nucleic Acids Res.* **42**, e133. doi:10.1093/nar/gku631
- Shekhar, K., Lapan, S. W., Whitney, I. E., Tran, N. M., Macosko, E. Z., Kowalczyk, M., Adiconis, X., Levin, J. Z., Nemesh, J., Goldman, M. et al. (2016). Comprehensive classification of retinal bipolar neurons by single-cell transcriptomics. *Cell* **166**, 1308-1323. doi:10.1016/j.cell.2016.07.054
- Stuart, T., Butler, A., Hoffman, P., Hafemeister, C., Papalexi, E., Mauck, W. M., III, Hao, Y., Stoeckius, M., Smibert, P. and Satija, R. (2019). Comprehensive integration of single-cell data. *Cell* **177**, 1888-1902. doi:10.1016/j.cell.2019.05.031
- Todd, L. and Fischer, A. J. (2015). Hedgehog signaling stimulates the formation of proliferating Müller glia-derived progenitor cells in the chick retina. *Development* **142**, 2610-2622. doi:10.1242/dev.121616
- Todd, L., Suarez, L., Quinn, C. and Fischer, A. J. (2018). Retinoic acid-signaling regulates the proliferative and neurogenic capacity of Müller glia-derived progenitor cells in the avian retina. *Stem Cells* **36**, 392-405. doi:10.1002/stem.2742
- Trompeter, H.-I., Abbadi, H., Iwaniuk, K. M., Hafner, M., Renwick, N., Tuschl, T., Schira, J., Müller, H. W. and Wernet, P. (2011). MicroRNAs MiR-17, MiR-20a, and MiR-106b act in concert to modulate E2F activity on cell cycle arrest during neuronal lineage differentiation of USSC. *PLoS ONE* **6**, e16138. doi:10.1371/journal.pone.0016138
- Ueki, Y., Karl, M. O., Sudar, S., Pollak, J., Taylor, R. J., Loeffler, K., Wilken, M. S., Reardon, S. and Reh, T. A. (2012). P53 is required for the developmental restriction in Müller glial proliferation in mouse retina. *Glia* **60**, 1579-1589. doi:10.1002/glia.22377
- Ueki, Y., Wilken, M. S., Cox, K. E., Chipman, N., Jorstad, N., Sternhagen, K., Simic, M., Ullom, K., Nakafuku, M. and Reh, T. A. (2015). Transgenic expression of the proneural transcription factor Ascl1 in Müller glia stimulates retinal regeneration in young mice. *Proc. Natl. Acad. Sci. USA* **112**, 13717-13722. doi:10.1073/pnas.1510595112
- Vázquez-Chona, F. R., Clark, A. M. and Levine, E. M. (2009). Rlbp1 promoter drives robust Müller glial GFP expression in transgenic mice. *Invest. Ophthalmol. Vis. Sci.* **50**, 3996-4003. doi:10.1167/iovs.08-3189
- Victor, M. B., Richner, M., Hermansteyne, T. O., Ransdell, J. L., Sobieski, C., Deng, P.-Y., Klyachko, V. A., Nerbonne, J. M. and Yoo, A. S. (2014). Generation of human striatal neurons by microRNA-dependent direct conversion of fibroblasts. *Neuron* **84**, 311-323. doi:10.1016/j.neuron.2014.10.016
- Visvanathan, J., Lee, S., Lee, B., Lee, J. W. and Lee, S.-K. (2007). The microRNA miR-124 antagonizes the anti-neural REST/SCP1 pathway during embryonic CNS development. *Genes Dev.* **21**, 744-749. doi:10.1101/gad.1519107
- Wernig, M., Zhao, J.-P., Pruszak, J., Hedlund, E., Fu, D., Soldner, F., Broccoli, V., Constantine-Paton, M., Isacson, O. and Jaenisch, R. (2008). Neurons derived from reprogrammed fibroblasts functionally integrate into the fetal brain and improve symptoms of rats with Parkinson's disease. *Proc. Natl. Acad. Sci. USA* **105**, 5856-5861. doi:10.1073/pnas.0801677105
- Wilken, M. S. and Reh, T. A. (2016). Retinal regeneration in birds and mice. *Curr. Opin. Genet. Dev.* **40**, 57-64. doi:10.1016/j.gde.2016.05.028
- Wohl, S. G. and Reh, T. A. (2016a). The microRNA expression profile of mouse Müller glia in vivo and in vitro. *Sci. Rep.* **6**, 35423. doi:10.1038/srep35423
- Wohl, S. G. and Reh, T. A. (2016b). miR-124-9-9* potentiates Ascl1-induced reprogramming of cultured Müller glia. *Glia* **64**, 743-762. doi:10.1002/glia.22958
- Wohl, S. G., Jorstad, N. L., Levine, E. M. and Reh, T. A. (2017). Müller glial microRNAs are required for the maintenance of glial homeostasis and retinal architecture. *Nat. Commun.* **8**, 1603. doi:10.1038/s41467-017-01624-y
- Worringer, K. A., Rand, T. A., Hayashi, Y., Sami, S., Takahashi, K., Tanabe, K., Narita, M., Srivastava, D. and Yamanaka, S. (2014). The let-7/LIN-41 pathway regulates reprogramming to human induced pluripotent stem cells by controlling expression of proliferation genes. *Cell Stem Cell* **14**, 40-52. doi:10.1016/j.stem.2013.11.001
- Xia, X. and Ahmad, I. (2016). let-7 microRNA regulates neurogenesis in the mammalian retina through Hmga2. *Dev. Biol.* **410**, 70-85. doi:10.1016/j.ydbio.2015.12.010
- Xiang, L., Chen, X.-J., Wu, K.-C., Zhang, C.-J., Zhou, G.-H., Lv, J.-N., Sun, L.-F., Cheng, F.-F., Cai, X.-B. and Jin, Z.-B. (2017). miR-183/96 plays a pivotal regulatory role in mouse photoreceptor maturation and maintenance. *Proc. Natl. Acad. Sci. USA* **114**, 6376-6381. doi:10.1073/pnas.1618757114
- Xu, S., Witmer, P. D., Lumayag, S., Kovacs, B. and Valle, D. (2007). MicroRNA (miRNA) transcriptome of mouse retina and identification of a sensory organ-specific miRNA cluster. *J. Biol. Chem.* **282**, 25053-25066. doi:10.1074/jbc.M700501200
- Xue, Y., Ouyang, K., Huang, J., Zhou, Y., Ouyang, H., Li, H., Wang, G., Wu, Q., Wei, C., Bi, Y. et al. (2013). Direct conversion of fibroblasts to neurons by reprogramming PTB-regulated microRNA circuits. *Cell* **152**, 82-96. doi:10.1016/j.cell.2012.11.045
- Yang, P., Cai, L., Zhang, G., Bian, Z. and Han, G. (2017). The role of the miR-17-92 cluster in neurogenesis and angiogenesis in the central nervous system of adults. *J. Neurosci. Res.* **95**, 1574-1581. doi:10.1002/jnr.23991
- Yao, K., Qiu, S., Tian, L., Snider, W. D., Flannery, J. G., Schaffer, D. V. and Chen, B. (2016). Wnt regulates proliferation and neurogenic potential of Müller glial cells via a Lin28/let-7 microRNA-dependent pathway in adult mammalian retinas. *Cell Rep.* **17**, 165-178. doi:10.1016/j.celrep.2016.08.078
- Yoo, A. S., Staahl, B. T., Chen, L. and Crabtree, G. R. (2009). MicroRNA-mediated switching of chromatin-remodelling complexes in neural development. *Nature* **460**, 642-646. doi:10.1038/nature08139
- Yoo, A. S., Sun, A. X., Li, L., Shcheglovitov, A., Portmann, T., Li, Y., Lee-Messer, C., Dolmetsch, R. E., Tsien, R. W. and Crabtree, G. R. (2011). MicroRNA-mediated conversion of human fibroblasts to neurons. *Nature* **476**, 228-231. doi:10.1038/nature10323
- Yoshida, A., Fujiwara, T., Uotani, K., Morita, T., Kiyono, M., Yokoo, S., Hasei, J., Nakata, E., Kunisada, T. and Ozaki, T. (2018). Clinical and functional significance of intracellular and extracellular microRNA-25-3p in osteosarcoma. *Acta Med. Okayama* **72**, 165-174. doi:10.1038/s41598-017-12660-5
- Yu, J., Vodyanik, M. A., Smuga-Otto, K., Antosiewicz-Bourget, J., Frane, J. L., Tian, S., Nie, J., Jonsdottir, G. A., Ruotti, V., Stewart, R. et al. (2007). Induced pluripotent stem cell lines derived from human somatic cells. *Science* **318**, 1917-1920. doi:10.1126/science.1151526
- Zelinka, C. P., Volkov, L., Goodman, Z. A., Todd, L., Palazzo, I., Bishop, W. A. and Fischer, A. J. (2016). mTOR signaling is required for the formation of proliferating Müller glia-derived progenitor cells in the chick retina. *Development* **143**, 1859-1873. doi:10.1242/dev.133215
- Zhang, J., Taylor, R. J., La Torre, A., Wilken, M. S., Cox, K. E., Reh, T. A. and Vetter, M. L. (2015). Ezh2 maintains retinal progenitor proliferation, transcriptional integrity, and the timing of late differentiation. *Dev. Biol.* **403**, 128-138. doi:10.1016/j.ydbio.2015.05.010
- Zhu, Q., Sun, W., Okano, K., Chen, Y., Zhang, N., Maeda, T. and Palczewski, K. (2011). Sponge transgenic mouse model reveals important roles for the microRNA-183 (miR-183)/96/182 cluster in postmitotic photoreceptors of the retina. *J. Biol. Chem.* **286**, 31749-31760. doi:10.1074/jbc.M111.259028



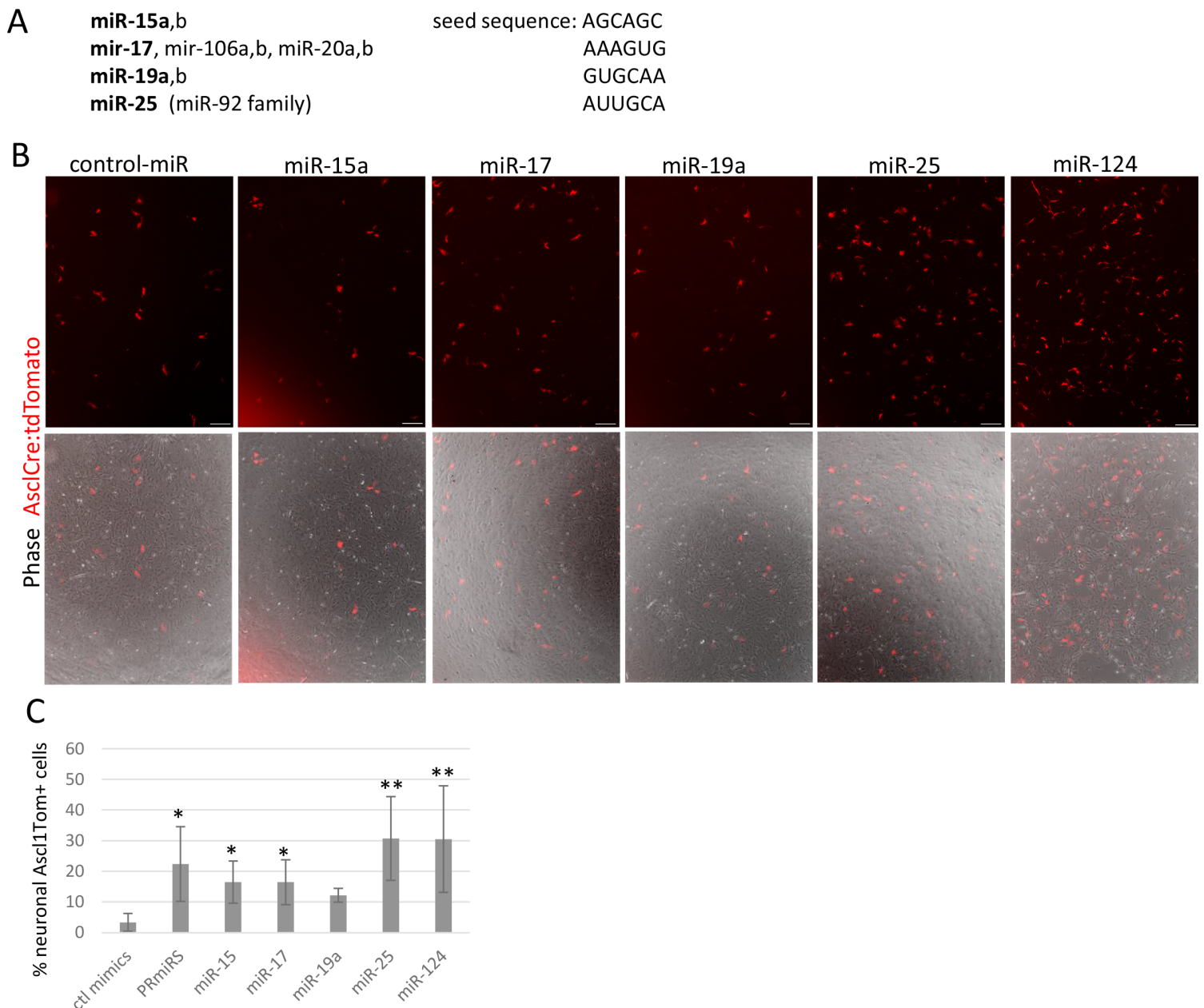


Figure S2: Overexpression of RPC-miRNAs induce Ascl1 expression in Müller glia

A: RPC-miRs with same seed sequence with chosen candidate in bolt. B: Live images of tdTomato+ cells after transfection with control, miR-15a, miR-17, miR-19, miR-25, and miR-124 mimic and 4 days post transfection. C: Number of Ascl1tdTomato+ cells with neuronal morphology 3-5 days post transfection, $n \geq 3$. Scale bars 200 μm . Significant differences are indicated: * $P < 0.05$, ** $P < 0.01$, ***, Mann-Whitney-test and Holm-Bonferroni correction.

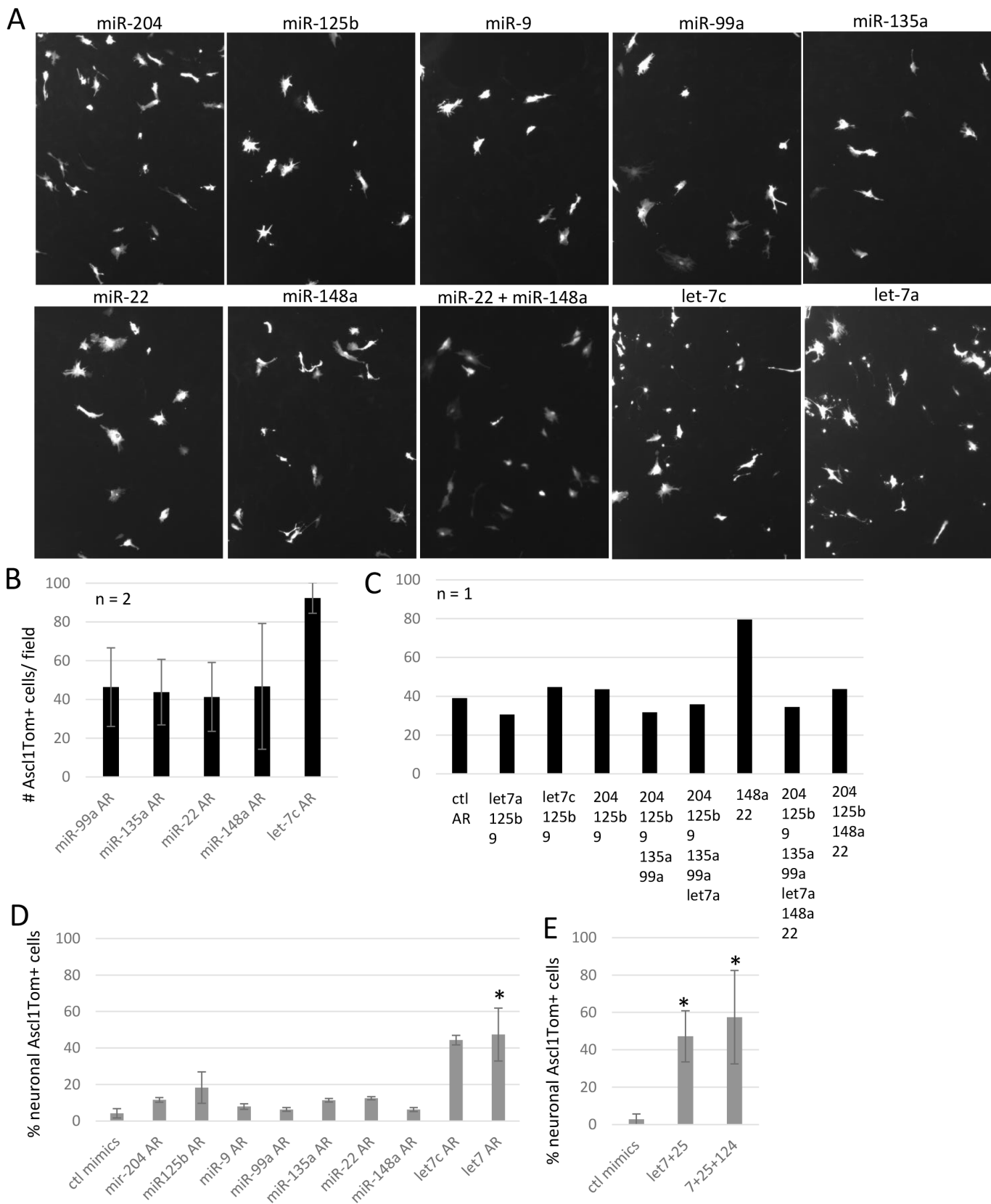


Figure S3: Antagonizing let-7 induces Ascl1 expression in Müller glia.

A: Live images of tdTomato+ cells after transfection with control, miR-204, miR-125b, miR-9, miR-99a, miR-135a, miR-22, miR-148, miR-22 and miR-148a, let-7c and let-7a antagonomiRs (AR) 9 days post transfection (dpTF). B,C: Number of Ascl1tdTomato+ cells per field 3-5d pTF. D: Number of Ascl1tdTomato+ cells with neuronal morphology 3-9 dpTF n ≥ 3, for miR-99a, 135a, 22, 148a and let-7c n = 2). Scale bars 100 μm. Significant differences are indicated *: p < 0.05, ** P < 0.01, ***: P < 0.001, Mann-Whitney-test and Holm-Bonferroni correction.

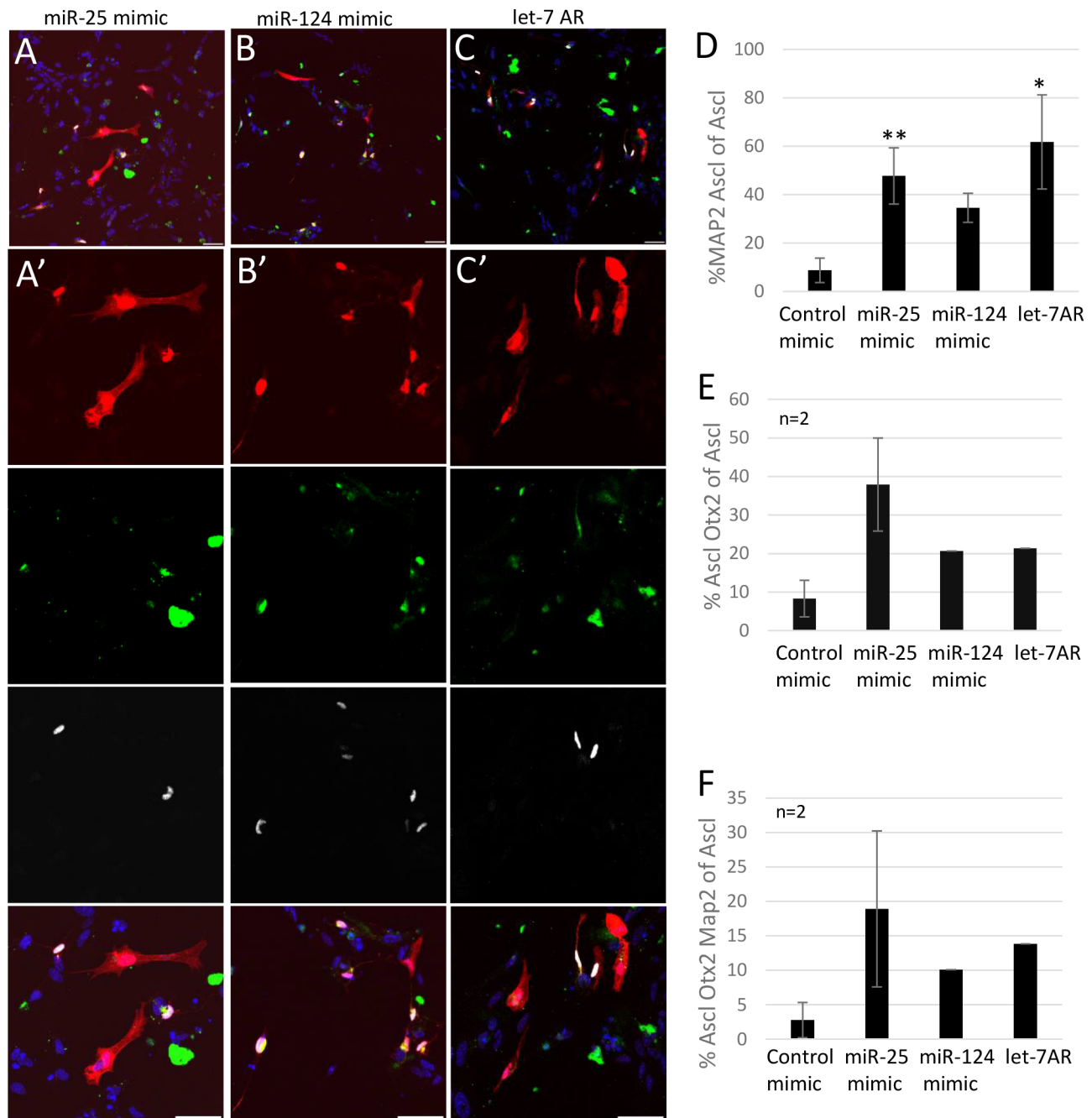


Figure S4: miR-25/miR-124/let-7 reprogrammed Ascl1 expressing Müller glia express Map2 and Otx2

A/A'-C/C': Immunofluorescent labeling with antibodies against tdTomato (AsclTom), Map2, and Otx2 as well as DAPI nuclear labeling 7 days post transfection (7dptf). D: Percentage of AsclTom+Map2+ cells of total AsclTom+ cells 7 dptf. E: Percentage of AsclTom+Otx2+ cells of total AsclTom+ cells 7 days post transfection. F: Percentage of AsclTom+Otx2+Map2+ cells of total AsclTom+ cells 7 dptf. Scale bars 100 μ m. Significant differences are indicated *: $p < 0.05$, ** $P < 0.01$, ***: $P < 0.001$, Mann-Whitney-test and Holm-Bonferroni correction.

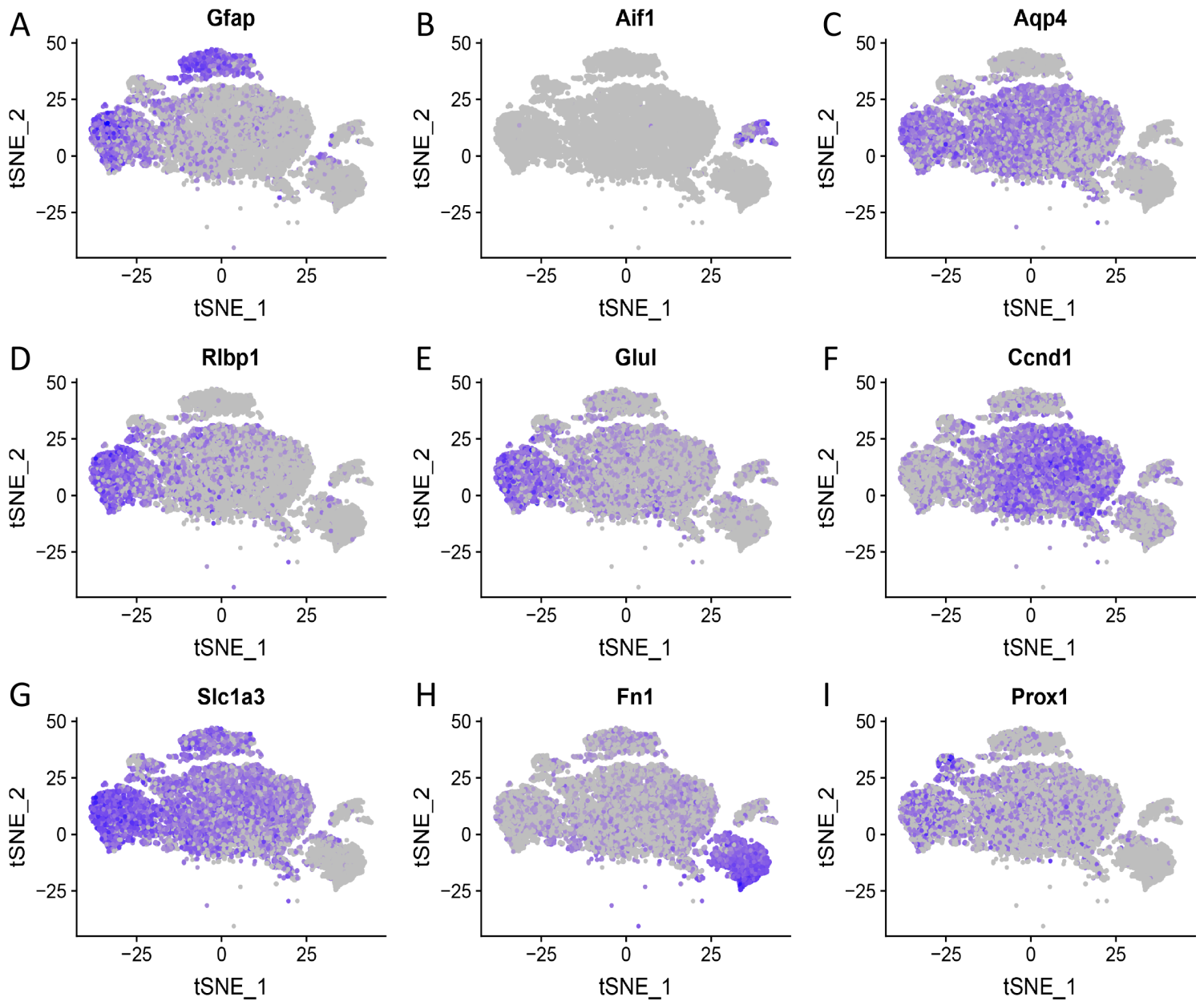


Figure S5: Identification of clusters.

tSNE plots for glial fibrillary acidic protein (GFAP) identifies astrocytes (A), allograft inflammatory factor (Aif1) microglia (B), aquaporin 4 (Aqp4, C), retinaldehyde binding protein 1 (Rlb1p1, D), glutamine synthetase (Glul, E) and Cyclin D1 (Ccnd1, F), and glutamate aspartate transporter (GLAST, Slc1a3, G) Müller glia, fibronectin1 (Fn1, H) endothelial cells/fibroblasts, and prospero homeobox protein1 (Prox1, I) progenitors and neurons.

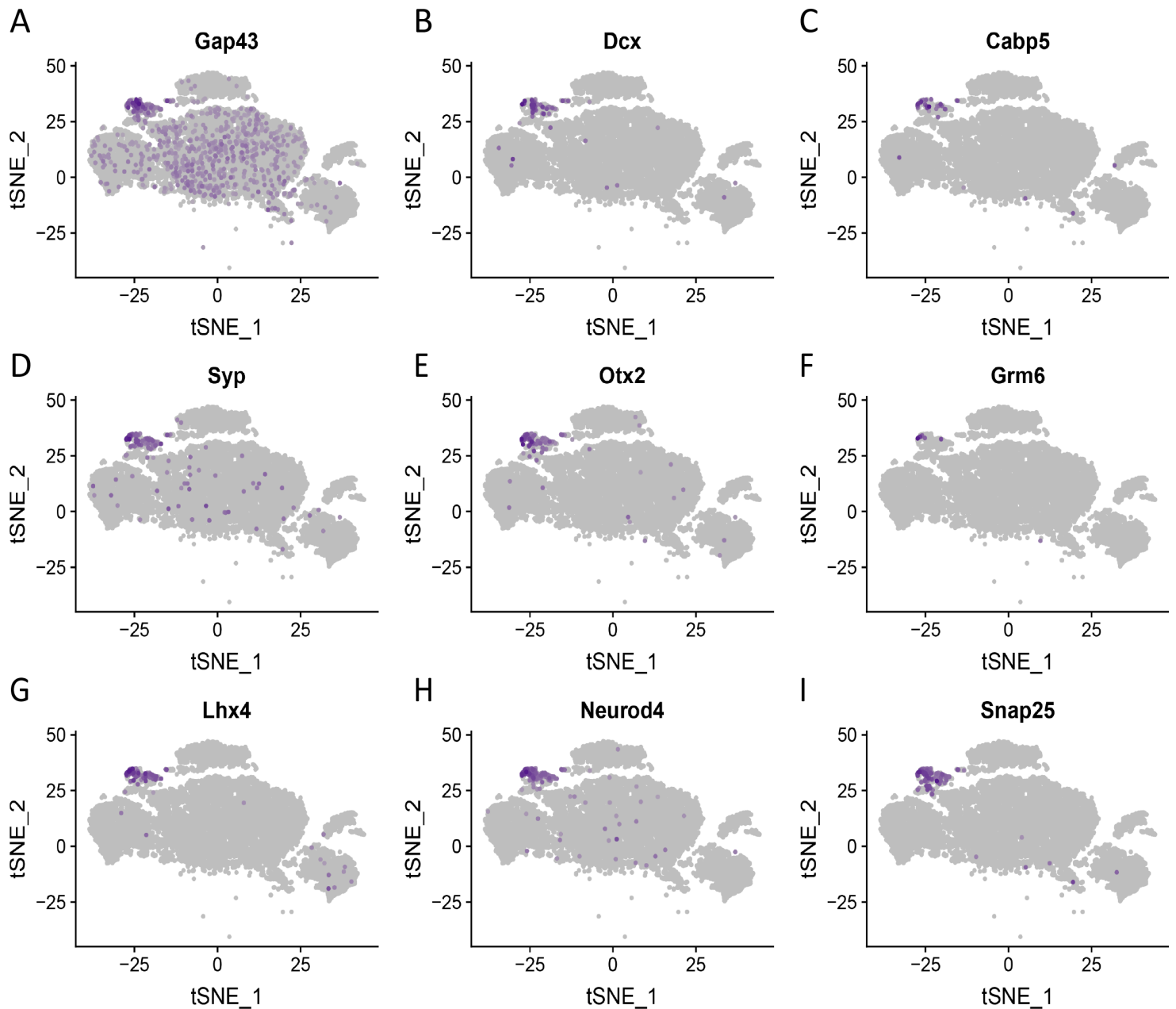


Figure S6: Neuronal marker expression in reprogrammed neurons after miR-25/124 mimic and let-7AR treatment.

tSNE plots for growth associated protein 43 (Gap43, A), doublecortin (Dcx, B), calcium binding protein 5 (Cabp5, C), synaptophysin (Syp, D), orthodenticle homeobox 2 (Otx2, E), glutamate metabotropic receptor 6 (Grm6, F), lim homeobox 4 (Lhx4, G), neuronal differentiation 4 (NeuroD4, H), and synapto-somal-associated protein 25 (Snap 25, I) dominate all in the neuronal cluster.

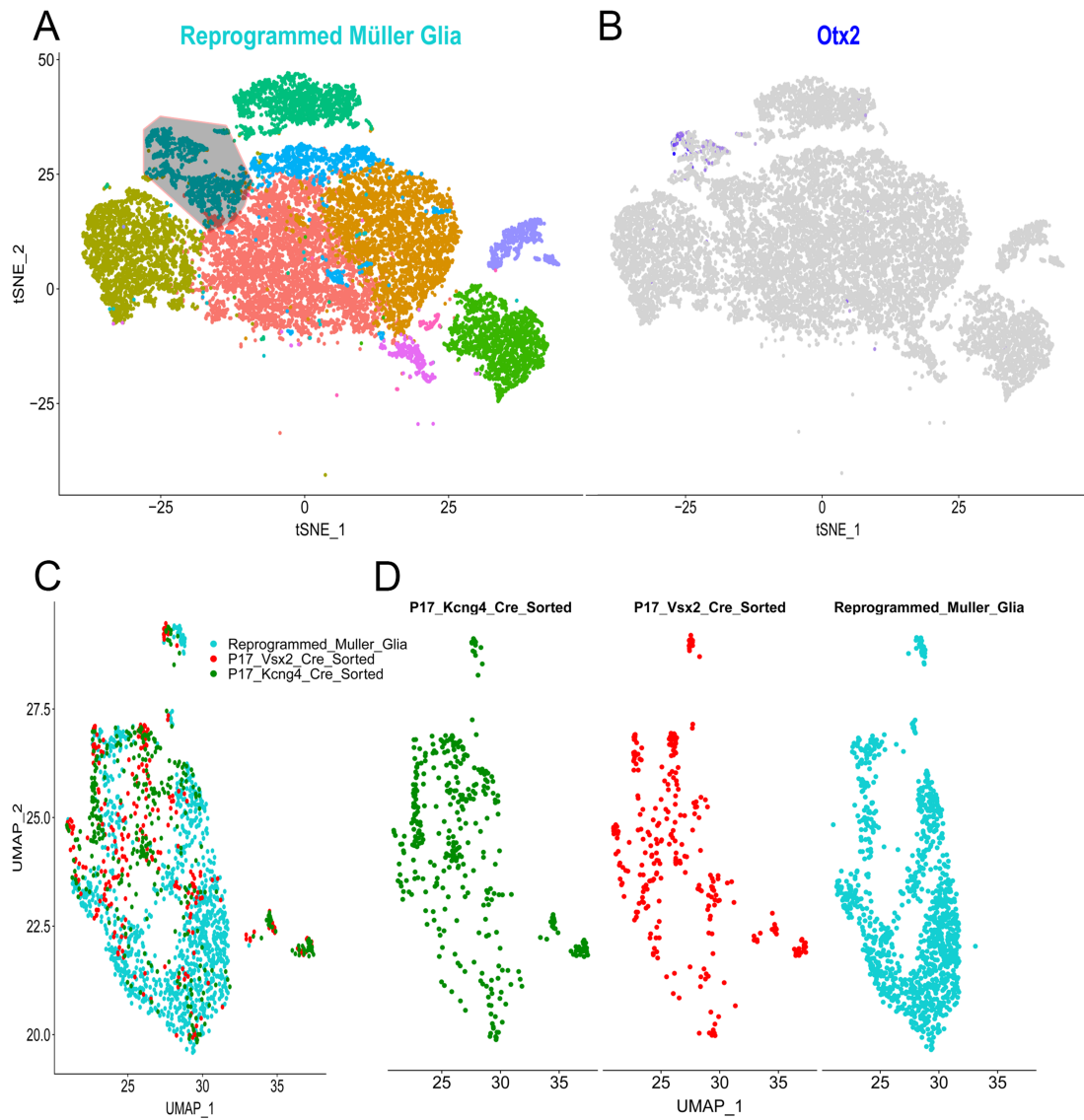


Figure S7. Comparison of gene expression between reprogrammed Müller glia and bipolar cells.

A: Plot showing the neuronal cluster of cells used for comparison with sorted bipolar cells from (Shekhar et al., 2016). B: Featureplot showing *Otx2* expression in the cluster in (A). C,D: Integration of reprogrammed Müller glia with sorted bipolar cell data merged (C) and contribution from individual groups (D).

Table S1: heat map clusters miRNAs (listed by name)

Green: moderate expression	Blue: low expression	Pink: high expression
mmu-miR-1	mmu-miR-101a	mmu-let-7a
mmu-miR-101b	mmu-miR-10a	mmu-let-7b
mmu-miR-105	mmu-miR-1188	mmu-let-7c
mmu-miR-107	mmu-miR-1193	mmu-let-7d
mmu-miR-1186b	mmu-miR-1194	mmu-let-7e
mmu-miR-1187	mmu-miR-1195	mmu-let-7f
mmu-miR-1190	mmu-miR-1306	mmu-let-7g
mmu-miR-1196	mmu-miR-135b	mmu-let-7i
mmu-miR-1197	mmu-miR-151-3p	mmu-miR-100
mmu-miR-1198	mmu-miR-182	mmu-miR-103
mmu-miR-125a-3p	mmu-miR-1839-3p	mmu-miR-106a+ miR-17
mmu-miR-125b-3p	mmu-miR-186	mmu-miR-106b
mmu-miR-127	mmu-miR-188-3p	mmu-miR-1186
mmu-miR-128	mmu-miR-1893	mmu-miR-1224
mmu-miR-129-5p	mmu-miR-1894-5p	mmu-miR-124
mmu-miR-132	mmu-miR-1895	mmu-miR-125a-5p
mmu-miR-133a	mmu-miR-1898	mmu-miR-125b-5p
mmu-miR-133b	mmu-miR-18a	mmu-miR-126-3p
mmu-miR-134	mmu-miR-1901	mmu-miR-129-3p
mmu-miR-136	mmu-miR-1903	mmu-miR-130a
mmu-miR-137	mmu-miR-190b	mmu-miR-130b
mmu-miR-138	mmu-miR-1928	mmu-miR-135a
mmu-miR-139-5p	mmu-miR-1939	mmu-miR-140
mmu-miR-142-3p	mmu-miR-1941-3p	mmu-miR-142-5p
mmu-miR-145	mmu-miR-1941-5p	mmu-miR-148a
mmu-miR-146a	mmu-miR-1943	mmu-miR-148b
mmu-miR-146b	mmu-miR-1946a	mmu-miR-151-5p
mmu-miR-149	mmu-miR-1967	mmu-miR-152
mmu-miR-150	mmu-miR-196b	mmu-miR-15a
mmu-miR-154	mmu-miR-1981	mmu-miR-15b
mmu-miR-181b+ miR-181d	mmu-miR-1983	mmu-miR-16
mmu-miR-1839-5p	mmu-miR-199a-3p	mmu-miR-181a
mmu-miR-184	mmu-miR-199a-5p	mmu-miR-181c
mmu-miR-185	mmu-miR-207	mmu-miR-183
mmu-miR-187	mmu-miR-212	mmu-miR-1900
mmu-miR-1892	mmu-miR-2134	mmu-miR-191
mmu-miR-1896	mmu-miR-2135	mmu-miR-1927
mmu-miR-190	mmu-miR-2137	mmu-miR-1937a+ miR-1937b
mmu-miR-1904	mmu-miR-2139	mmu-miR-1937c
mmu-miR-1906	mmu-miR-2145	mmu-miR-1944
mmu-miR-192	mmu-miR-216b	mmu-miR-1960
mmu-miR-1929	mmu-miR-218	mmu-miR-1965
mmu-miR-1933-5p	mmu-miR-2183	mmu-miR-1966
mmu-miR-193b	mmu-miR-221	mmu-miR-19a
mmu-miR-194	mmu-miR-2861	mmu-miR-19b

mmu-miR-1940	mmu-miR-290-5p	mmu-miR-204
mmu-miR-1942	mmu-miR-291a-3p	mmu-miR-20a+ miR-20b
mmu-miR-1945	mmu-miR-297c	mmu-miR-21
mmu-miR-195	mmu-miR-324-5p	mmu-miR-210
mmu-miR-1951	mmu-miR-331-5p	mmu-miR-2141
mmu-miR-1952	mmu-miR-337-3p	mmu-miR-22
mmu-miR-1955	mmu-miR-337-5p	mmu-miR-23a
mmu-miR-1956	mmu-miR-342-5p	mmu-miR-23b
mmu-miR-1959	mmu-miR-346	mmu-miR-25
mmu-miR-1961	mmu-miR-3474	mmu-miR-26b
mmu-miR-1964	mmu-miR-362-5p	mmu-miR-27a
mmu-miR-1968	mmu-miR-369-5p	mmu-miR-28
mmu-miR-200a	mmu-miR-376a	mmu-miR-29a
mmu-miR-200b	mmu-miR-377	mmu-miR-29c
mmu-miR-200c	mmu-miR-380-5p	mmu-miR-301a
mmu-miR-201	mmu-miR-410	mmu-miR-30a
mmu-miR-202-3p	mmu-miR-421	mmu-miR-30b
mmu-miR-202-5p	mmu-miR-448	mmu-miR-30c
mmu-miR-203	mmu-miR-449a	mmu-miR-30d
mmu-miR-205	mmu-miR-455	mmu-miR-322
mmu-miR-206	mmu-miR-466c-5p	mmu-miR-335-5p
mmu-miR-208a	mmu-miR-466l	mmu-miR-340-5p
mmu-miR-211	mmu-miR-487b	mmu-miR-342-3p
mmu-miR-2138	mmu-miR-488	mmu-miR-350
mmu-miR-2140	mmu-miR-491	mmu-miR-425
mmu-miR-2146	mmu-miR-493	mmu-miR-532-5p
mmu-miR-24	mmu-miR-500	mmu-miR-674
mmu-miR-26a	mmu-miR-501-3p	mmu-miR-720
mmu-miR-27b	mmu-miR-504	mmu-miR-872
mmu-miR-290-3p	mmu-miR-542-3p	mmu-miR-9
mmu-miR-296-5p	mmu-miR-543	mmu-miR-93
mmu-miR-29b	mmu-miR-665	mmu-miR-96
mmu-miR-300	mmu-miR-668	mmu-miR-98
mmu-miR-301b	mmu-miR-669e	mmu-miR-99a
mmu-miR-30e	mmu-miR-669i	mmu-miR-99b
mmu-miR-31	mmu-miR-669o	
mmu-miR-32	mmu-miR-675-5p	
mmu-miR-320	mmu-miR-678	
mmu-miR-323-3p	mmu-miR-682	
mmu-miR-323-5p	mmu-miR-683	
mmu-miR-328	mmu-miR-694	
mmu-miR-329	mmu-miR-701	
mmu-miR-33	mmu-miR-706	
mmu-miR-330	mmu-miR-759	
mmu-miR-331-3p	mmu-miR-760	
mmu-miR-335-3p	mmu-miR-764-3p	
mmu-miR-338-3p	mmu-miR-770-3p	
mmu-miR-338-5p	mmu-miR-770-5p	
mmu-miR-340-3p	mmu-miR-804	

mmu-miR-345-5p	mmu-miR-875-3p	
mmu-miR-3470a+ miR-3470b	mmu-miR-875-5p	
mmu-miR-3471	mmu-miR-877	
mmu-miR-3472	mmu-miR-879	
mmu-miR-34a	mmu-miR-881	
mmu-miR-34b-3p	mmu-miR-883a-3p	
mmu-miR-34b-5p	mmu-miR-883b-5p	
mmu-miR-361	mmu-miR-92a	
mmu-miR-362-3p	mmu-miR-92b	
mmu-miR-365		
mmu-miR-367		
mmu-miR-369-3p		
mmu-miR-370		
mmu-miR-374		
mmu-miR-376b		
mmu-miR-376c		
mmu-miR-378		
mmu-miR-381		
mmu-miR-382		
mmu-miR-384-3p		
mmu-miR-384-5p		
mmu-miR-423-3p		
mmu-miR-423-5p		
mmu-miR-431		
mmu-miR-432		
mmu-miR-433		
mmu-miR-434-3p		
mmu-miR-434-5p		
mmu-miR-450a-5p		
mmu-miR-463		
mmu-miR-466a-3p		
mmu-miR-466g		
mmu-miR-467a		
mmu-miR-467e		
mmu-miR-467f		
mmu-miR-467h+ miR- 669d+ miR-669l		
mmu-miR-468		
mmu-miR-484		
mmu-miR-485		
mmu-miR-490		
mmu-miR-495		
mmu-miR-497		
mmu-miR-501-5p		
mmu-miR-505		
mmu-miR-509-5p		
mmu-miR-532-3p		
mmu-miR-539		

mmu-miR-541		
mmu-miR-542-5p		
mmu-miR-551b		
mmu-miR-574-3p		
mmu-miR-574-5p		
mmu-miR-582-5p		
mmu-miR-590-5p		
mmu-miR-652		
mmu-miR-654-3p		
mmu-miR-666-3p		
mmu-miR-669a		
mmu-miR-669f		
mmu-miR-669j		
mmu-miR-670		
mmu-miR-671-3p		
mmu-miR-672		
mmu-miR-676		
mmu-miR-688		
mmu-miR-690		
mmu-miR-695		
mmu-miR-708		
mmu-miR-709		
mmu-miR-710		
mmu-miR-714		
mmu-miR-717		
mmu-miR-741		
mmu-miR-742		
mmu-miR-761		
mmu-miR-762		
mmu-miR-764-5p		
mmu-miR-767		
mmu-miR-7a		
mmu-miR-7b		
mmu-miR-871		
mmu-miR-873		
mmu-miR-876-3p		
mmu-miR-882		
mmu-miR-883a-5p		

Table S2: miRNA counts normalized for all ages sorted after highly expressed miRs in P2 RPC (top 25).

miR	Sample ID	P2 RPC	P8 MG	P11 MG	Adult MG
mmu-miR-9	MIMAT0000142	63981	100674	89452	65337
mmu-miR-16	MIMAT0000527	35845	17228	11079	6325
mmu-miR-720	MIMAT0003484	26466	12637	10414	20736
mmu-miR-204	MIMAT0000237	25967	55841	99116	247414
mmu-miR-181a	MIMAT0000210	25080	26599	29255	42317
mmu-miR-20a+mmu-miR-20b	MIMAT0000529	21395	6251	1991	316
mmu-miR-25	MIMAT0000652	20511	7005	3250	2080
mmu-miR-15b	MIMAT0000124	20032	5859	3089	847
mmu-let-7g	MIMAT0000121	15750	14952	14317	13583
mmu-let-7d	MIMAT0000383	15516	15155	14853	11549
mmu-miR-106a+mmu-miR-17	MIMAT0000385	13999	4507	1418	275
mmu-miR-96	MIMAT0000541	12811	3445	629	285
mmu-let-7i	MIMAT0000122	12334	10505	7160	2148
mmu-miR-125a-5p	MIMAT0000135	9841	8497	6348	4921
mmu-let-7a	MIMAT0000521	9477	8259	8728	7077
mmu-miR-15a	MIMAT0000526	8593	3318	1678	475
mmu-miR-1944	MIMAT0009409	8207	5147	5477	4389
mmu-miR-183	MIMAT0000212	7352	2111	543	353
mmu-let-7c	MIMAT0000523	7030	17538	26463	22705
mmu-miR-124	MIMAT0000134	7015	3117	1220	1211
mmu-let-7b	MIMAT0000522	6889	15605	19881	15661
mmu-miR-19a	MIMAT0000651	6501	999	389	120
mmu-miR-125b-5p	MIMAT0000136	4547	22081	30204	94931
mmu-miR-301a	MIMAT0000379	4339	908	533	658
mmu-miR-30c	MIMAT0000514	4087	3372	3776	12121

Table S3: genotyping primers

Gene name	Forward sequence (5' to 3')	Reverse sequence (3' to 5')
<i>Ascl1Cre knock in</i> <i>Generic cre primers</i>	TGCCAGGATCAGGGTTAAAG	TCCTTAGCGCCGTAAATCAA
<i>Sox2Cre knock in</i> <i>Generic cre primers</i>	TGCCAGGATCAGGGTTAAAG	TCCTTAGCGCCGTAAATCAA
<i>Rlbp1Cre transgene</i>	CAAGTGTGAGAGACAGCATTG	TCCTTAGCGCCGTAAATCAA
<i>tdTomato wildtype</i>	AAG GGA GCT GCA GTG GAG TA	CCG AAA ATC TGT GGG AAG TC
<i>tdTomato mutant</i>	CTG TTC CTG TAC GGC ATG G	GGC ATT AAA GCA GCG TAT CC

Table S4: mimics and antagomiRs (AR)

name	Catalog number
<i>Control mimic</i>	CN-001000-01-50
<i>Control antagomiR (AR)</i>	IN-001005-01-05
<i>miR-15a-5p mimic</i>	C-310510-05-0020
<i>miR-17-5p mimic</i>	C-310561-07-0020
<i>miR-19a-3p mimic</i>	C-310563-05-0020
<i>miR-25-3p mimic</i>	C-310564-05-0020
<i>miR-124-3p mimic</i>	C-310390-05-0020
<i>miR-204-5p AR</i>	IH-310460-08-0005
<i>miR-125b-5pAR</i>	IH-310393-07-0050
<i>miR-9-5p AR</i>	IH-310402-08-0005
<i>let-7a-5p AR</i>	IH-310503-08-0050
<i>let-7c-5p AR</i>	IH-310506-07-0005
<i>miR-135a-5p AR</i>	IH-310411-07-0005
<i>miR-99a-5p AR</i>	IH-310386-08-0005
<i>miR-22-3p AR</i>	IH-310516-07-0005
<i>miR-148a-3p AR</i>	IH-310496-07-0005

Table S5: primary antibodies

antibody	concentration	Company, Catalog #
rat anti RFP (tdTomato)	1:500	Antibodies online, ABIN334653
mouse anti glutamine synthetase (GS)	1:200	Millipore, MAB 302
rabbit anti Sox9	1:1000	Millipore, AB5535
goat anti Sox2 (Y-17)	1:100	Santa Cruz, sc-17320
mouse anti Map2	1:200	Sigma, M4403
mouse anti TUJ1	1:1000	Covance, MMS-435P
goat anti Otx2	1:200	R&D Systems, BAF1979
rabbit anti Pax6	1:500	Covance, PRB-278P

Table S6: secondary antibodies

antibody	concentration	Company, catalog #
Rhodamine Red 570 - AffiniPure F(ab') ₂ Fragment Donkey Anti-Rat IgG (H+L)	1:1000	Jackson ImmunoResearch Laboratories, Inc., 712-296-150
Alexa Fluor 488- AffiniPure F(ab') ₂ Fragment Donkey Anti-Mouse IgG (H+L)	1:500	Jackson ImmunoResearch Laboratories, Inc., 715-546-150
Alexa Fluor 488 - AffiniPure F(ab') ₂ Fragment Donkey Anti-Rabbit IgG (H+L)	1:500	Jackson ImmunoResearch Laboratories, Inc., 711-546-152
Alexa Fluor 488 - AffiniPure F(ab') ₂ Fragment Donkey Anti-Goat IgG (H+L)	1:500	Jackson ImmunoResearch Laboratories, Inc., 705-546-147
Alexa Fluor 647 - AffiniPure F(ab') ₂ Fragment Donkey Anti-Rabbit IgG (H+L)	1:500	Jackson ImmunoResearch Laboratories, Inc., 711-606-152
Alexa Fluor 647 - AffiniPure F(ab') ₂ Fragment Donkey Anti-Goat IgG (H+L)	1:500	Jackson ImmunoResearch Laboratories, Inc., 705-606-147